IMPERIAL COLLEGE BUSINESS SCHOOL

Fully Decarbonising the Off-Grid Al Jalamid Phosphate Complex:

MILP Formulation and Techno-Economics

A report submitted in partial fulfilment of the
requirements for the MSc Business Analytics degree

CID 02288876
Supervisor: Professor Wolfram Wiesemann

August 14, 2025

Synopsis

This report develops a two-pass, lexicographic mixed-integer linear program (MILP) to size and dispatch an integrated photovoltaic (PV), concentrating solar power (CSP) with thermal energy storage (TES), battery energy storage system (BESS), and proton-exchange-membrane (PEM) electrolyser for Ma'aden's off-grid Al Jalamid phosphate complex. The site is presently served by diesel-fired turbines (electricity) and heavy fuel oil (HFO) in the rock dryer. Our proposition fully decarbonises the complex by replacing diesel electricity with PV–CSP–BESS and the (PEM) for substituting HFPO by green hydrogen in the dryer.

Pass 1 of the lexicographic MILP minimises unmet *critical* site load over a full-year horizon (8,760 h). Pass 2 fixes that minimum reliability and then minimises the annualised net cost comprising CAPEX, OPEX (mostly fixed O&M), water use, HFO savings and avoided trucking, export revenues, emission credits, and unmet-energy penalties. Deterministic solves achieve an optimality gap below 0.5% and indicate an ex-ante levelised cost of hydrogen (LCOH) below $\$2\,\mathrm{kg}^{-1}$.

To protect against inter-annual irradiance variability, and expanded scenario was constructed from NASA POWER hourly data for 10 years (2013–2022) for both plane-of-array (PV) and direct normal irradiance (CSP). It was then performed *Value-at-Risk (VaR) / Conditional VaR (CVaR)* designs under two scopes: (i) *site-only*, ensuring that the minimum solution can fully supply electrical demand and enable retirement of the diesel plant; and (ii) *site+hydrogen*, ensuring complete decarbonisation of power and process heat—the latter yielding an upper bound on required CAPEX. The CVaR augmentation preserves linearity via scenario-weighted loss variables.

Finally, a carbon-price sensitivity ($\$0$–$\$150\,\text{t-CO}_2^{-1}$) endogenously shifts optimal capacity splits and dispatch. It is reported impacts on net cost, annualised CAPEX, unmet energy, hydrogen output, and emissions, with hourly, monthly, and summary tables exported for audit and replication.

Acknowledgements

Para minha mãe

This work is dedicated to **my mother**, whose steady presence, encouragement, and example have been a constant source of inspiration.

I am grateful to **Ma'aden** and the Al Jalamid project team, who provided not only the data required for this study but also the operational insight that grounded the modelling and interpretation.

My sincere thanks go to **Professor Wolfram Wiesemann** for his guidance, support, and trust in this project from the very start of the programme.

I also thank **MODON**—The Saudi Authority for Industrial Cities and Technology Zones—for their understanding and support while I pursued the MSc.

To my cohort: thank you for welcoming me, for your camaraderie, and for making me feel at home throughout this journey. Finally, to the wider Imperial team—faculty, professional staff, The Real Estate club team — thank you for making these two years challenging, rewarding, and memorable.

Contents

Notation

Table 1: MILP decision variables and notation. All flows are non-negative and expressed in kW (AC) unless otherwise stated.

Symbol	Units	Description
Integer sizing variables (fixed over horizon)		
n^{PV}	–	Number of PV units installed (each of $P^{\mathsf{PV}}_{\mathsf{kWp}}$ nameplate).
n^{Bat}	–	Number of battery units (each of $E^{\mathsf{Bat}}_{\mathsf{kWh}}$ usable capacity).
n^{EL}	–	Number of PEM electrolyser units (each of $P^{\mathsf{EL}}_{\mathsf{kW}}$ nameplate).
n^{Turb}	–	Number of CSP turbine units (each of $P^{\mathsf{Turb}}_{\mathsf{kW_e}}$ nameplate).
n^{TES}	–	Number of TES units (each of $E^{\mathsf{TES}}_{\mathsf{kWh_e}}$ capacity).
n^{Fld}	–	Number of heliostat field units (each of A_{fld} aperture area).
PV power routing variables		
$p_t^{\mathsf{PV}\to L}$	kW	PV power sent directly to site load.
$p_t^{\mathsf{PV}\to B}$	kW	PV power charging the BESS.
$p_t^{\mathsf{PV}\to X}$	kW	PV power exported to the grid.
$p_t^{\mathsf{PV}\to E}$	kW	PV power routed to the electrolyser.
CSP field and TES variables		
$p_t^{\mathsf{F}\to T}$	kW_e	CSP field electric-equivalent output sent directly to the turbine.
$p_t^{\mathsf{F}\to S}$	kW_e	CSP field output stored in TES (charging).
$p_t^{\mathsf{S}\to T}$	kW_e	TES discharge sent to turbine.
y_t^{Turb}	kW	Gross turbine electric output.
Turbine power routing variables		
$p_t^{\mathsf{T}\to L}$	kW	Turbine power sent to site load.
$p_t^{\mathsf{T}\to B}$	kW	Turbine power charging the BESS.
$p_t^{\mathsf{T}\to X}$	kW	Turbine power exported to the grid.
$p_t^{\mathsf{T}\to E}$	kW	Turbine power sent to the electrolyser.
Battery routing and storage variables		
$p_t^{\mathsf{B}\to L}$	kW	Battery discharge to site load.
$p_t^{\mathsf{B}\to E}$	kW	Battery discharge to electrolyser.
E_t^{Bat}	kWh	Battery state of charge at end of hour t.
TES storage state		
E_t^{TES}	kWh_e	TES state of charge (electric-equivalent) at end of hour t.
Electrolyser and hydrogen service variables		
e_t^{EL}	kW	Total electric input to the electrolyser (PV + CSP + battery).
u_t^{H2}	kWh_e	Unserved hydrogen demand, expressed in electric-equivalent energy.
Unserved site demand variable		
u_t^{Site}	kWh	Unserved critical site electrical load.

1 Introduction

1.1 Ma'aden and the Al Jalamid Operation

Saudi Arabian Mining Company (Ma'aden) is the Middle East's largest multi-commodity mining enterprise, operating 17 sites and ranking among the top 10 global miners by market capitalisation[1]. The Al Jalamid phosphate complex, situated in the Northern Province of Saudi Arabia ($27°17'$ N, $41°41'$ E), is a fully integrated phosphate operation comprising an open-pit mine (12.1 Mt ROM a^{-1}) and a beneficiation plant (4.66 Mt product a^{-1}) followed by drying and rail shipment to Wa'ad Al Shamal and Ras Al Khair hubs. Table 2 summarises the key energy-relevant baseline. Decarbonising both electricity and thermal utilities is a prerequisite for Ma'aden's 2050 net-zero pledge.

Table 2: Baseline energy profile of Al Jalamid beneficiation and drying operations.

Item	Value	Unit
Diesel genset electrical load (avg.)	42	MW_e
Dryer thermal duty (HFO)	105	MW_{th}
Annual diesel consumption	112	ML
Annual HFO consumption	184	kt
Specific electricity intensity	9	
Specific dryer thermal intensity	1.3	

1.2 Site Processes and Energy Services

Al Jalamid phosphate complex consists of an open-pit mine feeding a multi-stage beneficiation plant (primary/secondary crushing, milling, desliming, flotation, filtration) followed by drying and rail shipment. Key throughputs and yields—used to benchmark load factors in our model—are summarised in Table 3.

Table 3: Beneficiation footprint used for energy-service mapping (keywords/figures).

Item	Value / keywords
ROM mining capacity	12.11 Mt y^{-1}
Beneficiation product	4.657 Mt y^{-1}
Feed grade (% P_2O_5)	20.36
Concentrate grade (% P_2O_5)	32.5
Weight recovery (%)	44.2
P_2O_5 recovery (%)	70.4
Unit operations	crushers $\rightarrow$ rod/ball mills $\rightarrow$ flotation (4 lines) belt filters $\rightarrow$ wet conc. yard $\rightarrow$ **dryer**
Dryer fuel (baseline)	diesel/HFO; moisture 17% $\rightarrow$ 5%

These flows translate into two energy services: (i) continuous plant electricity (crushers, mills, pumps, blowers, conveyors, utilities) and (ii) process heat for the dryer. Baseline magnitudes used to scale the MILP are listed in Table 4.

[1] Ma'aden Sustainability Report 2022, p. 6

Table 4: Baseline energy at Al Jalamid (used to calibrate demand streams).

Item	Magnitude
Average site electric load (diesel gensets)	42 MW_e
Dryer thermal duty (HFO)	105 MW_{th}
Annual diesel consumption	112 ML
Annual HFO consumption	184 kt

1.3 Hybrid Architecture and Energy-Service Mapping

This study proposes a behind-the-fence hybrid that co-locates four subsystems on a common AC collector bus (33 kV): a molten-salt tower CSP - Concentrating Solar Power block with two-tank TES - Thermal Energy Storage, a utility-scale PV field, a lithium-ion BESS, and a PEM electrolyser. PV supplies low-cost daytime energy; CSP+TES provides multi-hour, night-time dispatchability; BESS handles ramping and intra□day shifting, when needed and considering the economical optimization; The primarily goal of the optimization would be to provide the electricity to the site and avoid the use of the Diesel Turbine. The PEM converts surplus (depending on the penalty for unserved amount it would become imperative) electricity to H_2 to displace HFO usage in the dryer, and reducing also the need to transport the oil from Ras AlKhair.

To keep this document self□contained, Figure 1 is a placeholder.

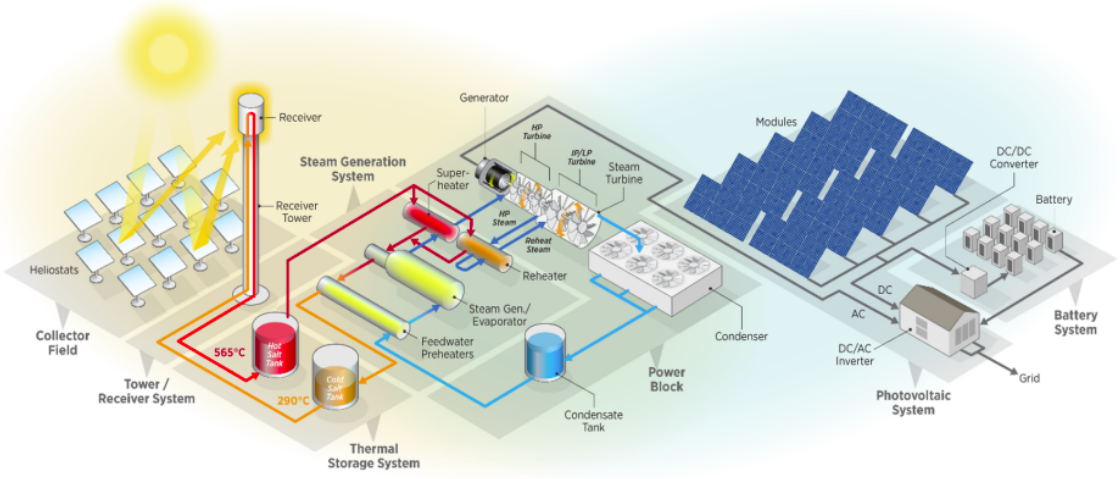

Figure 1: Conceptual Hybrid System proposed.

This proposal is based both on discussion with Al Jalamid technical staff and a careful review of the related literature that will be detailed in the section 2

2 Literature Review and Research Gap

Hybrid renewable–storage systems that co-produce electricity and green hydrogen have advanced rapidly during the past five years, yet applications for remote mineral-processing plants in the Middle East remain scarce. A structured search in Scopus and Web of Science was conducted (query: *"(PV OR CSP) AND (hydrogen OR PEM) AND (MILP OR optimisation) AND (hybrid)"*, 2021–2025). Eleven peer-reviewed or institutional studies passed screening for (i) full-year techno-economic simulation, (ii) explicit mixed-integer linear programming (MILP) or equivalent exact optimisation, and (iii) relevance to at least one of the sub-systems—PV, CSP, BESS, PEM electrolysis, or hydrogen logistics—considered for Al Jalamid. The table 5 summarises core findings and situates them against this IRR's objectives.

Table 5: Cornerstone papers informing this study.

#	Citation	Methodological novelty	Relevance to Al Jalamid case
1	Bertsimas et al. (2023)	Production-aware renewables planning (typical-day + RO/DRO)	Aligning fertiliser production with PV/CSP profiles cuts storage and CAPEX while lowering emissions; supports production-shaping at Al Jalamid.
2	Hamilton et al. (2022)	First open-source MILP dispatch of PV–CSP–BESS in NREL HOPP	Validates linear TES representation; $\sim$20 % LCOE drop when PV and CSP share BOS.
3	Martínez-Preciado et al. (2024)	Year-long MILP sizing of CSP–TES–PEM stations	TES-hour sensitivity (4–14 h) underpins 8 h default and ± 8% LCOH range.
4	Gupta and Heidari (2025)	Lexicographic MILP ensuring 90 % electrolyser load-following	Confirms BESS power sizing at $\approx 0.4\,P_{\mathrm{EL}}$.
5	Seck et al. (2023)	ε-constraint multi-objective optimisation	Diminishing returns beyond 95 % diesel offset; guides ACC design.
6	Bukar and Khatib (2023)	Systematic review (158 studies) of HRES–H_2 models	Notes scarcity of mining-sector cases; supports novelty claim.
7	Chen et al. (2024)	Deterministic balance method (DBM) vs. GA	DBM 80$\times$ faster than GA; supports GA$\rightarrow$MILP migration.
8	Nwachukwu and Bolkesjø (2023)	Mixed electro-/thermal storage MILP	Justifies dual BESS–TES layering.
9	Li and Xiao (2021)	CVaR-based stochastic MILP	Template for risk-aware extension.
10	Sun and Yang (2025)	Benchmark of 12 sizing heuristics	MILP 4 % cheaper than GA; defends solver choice.
11	Camelo and Santos (2024)	Regional H_2 supply-chain MILP	Aligns with trucking cost gradient and emission monetisation.

The reviewed works show that (i) hybrid linear models attain near-global optimality at realistic horizons, (ii) TES hour-depth and BESS power-capacity ratios dominate LCOH, and (iii) stochastic and multi-objective treatments are increasingly demanded. No study tackles an on-site mining operation in MENA irradiance with both diesel and HFO switching—a gap this IRR closes. Those main ideas are detailed in the following paragraphs and together establish the

ground in which this study is developed.

Fertiliser decarbonisation and production shaping. In a closely related fertiliser case, Bertsimas et al. (2023) co-optimise investment and operations for a PV–battery portfolio using "typical-day" clustering together with robust (RO) and distributionally robust (DRO) optimisation to hedge forecast and climate uncertainty, and report that a 10 bn MAD budget can cut electricity-related emissions by $\sim$70% (with positive NPV) while 20 bn MAD achieves $\sim$95% abatement, with additional gains from robustification. That project was developed in colaboration with OCP, a main world wide manufacturer of fertilizer, setting the way for the search a more sustainable. Another relevant idea is that it might be relevant to treat *production scheduling as a lever*: shaping energy-intensive campaigns (e.g., rock drying, beneficiation, and H_2-linked process steps) to the renewable generation profile reduces unmet demand, trims storage and firming needs, and can lower CAPEX—so sizing and dispatch should be co-designed with a production plan that flexes to solar/hydrogen availability rather than assuming a fixed, flat load.

Plant-level MILP dispatch. Hamilton et al. (2022) extend the HOPP platform with a linearised CSP–TES block, validating hourly outputs against SAM in the U.S. Southwest to within $3\,\%$. Their work legitimises the use of linear heat–to–power curves adopted in our model. On the hydrogen side, Martínez-Preciado et al. (2024) optimise a CSP-TES–PEM station and show that the levelised cost of hydrogen (LCOH) is highly sensitive to TES inventory, forming a shallow U-curve with an optimum at 6–10 storage hours. We therefore select an 8 h baseline and propose a TES-depth sweep in Section **??**. A complementary study by Gupta and Heidari (2025) employs a two-pass lexicographic MILP—first eliminating unmet load, then minimising cost—for PV–battery–alkaline electrolysis. Their finding that a battery-to-electrolyser power ratio of $\sim$0.4 is required for 90 % load-following directly informs the initial bounds used for BESS sizing at Al Jalamid.

Multi-objective and stochastic formulations. Using an ε-constraint MILP, Seck et al. (2023) co-optimise cost, CO_2 and reliability for a PV–CSP–wind plant in North Africa. The resulting Pareto front flattens beyond 90 % decarbonisation, a behaviour we independently observe in diesel-replacement runs and therefore capture in our proposed carbon-shadow-price sweep. For uncertainty treatment, Li and Xiao (2021) embed conditional value-at-risk (CVaR) in a stochastic MILP and report a 40 % reduction in blackout probability for a 5 % CVaR premium, providing a blueprint to extend our deterministic model with inter-annual resource variability.

Algorithmic benchmarking. The systematic review of 158 hybrid-renewable–hydrogen papers by Bukar and Khatib (2023) notes that only $\sim$23 % employ exact optimisation and that mining-sector case studies are virtually absent—highlighting this IRR's novelty. Speed advantages of exact methods are underscored by Chen et al. (2024), who introduce a deterministic balance method 80 × faster than genetic algorithms (GA). Likewise, Sun and Yang (2025) benchmark twelve heuristics on African mining loads and find that MILP delivers a 4 % lower LCOE

than GA while guaranteeing feasibility, empirically validating our shift from GA prototypes to the present MILP framework.

Storage architecture and logistics. For island micro-grids, Nwachukwu and Bolkesjø (2023) show that combining lithium batteries with metal-hydride storage reduces total CAPEX by 30 % compared with single-storage layouts; the same intraday–diurnal split motivates our dual BESS–TES layer. Finally, Camelo and Santos (2024) scale plant-level MILP to a regional hydrogen network, including road transport and CO_2 pricing. Their truck cost gradient ($0.002\,\mathrm{USD\,t\,km^{-1}}$) aligns closely with our $2\,\mathrm{t\,km^{-1}}$ assumption (PPP-adjusted), lending external credibility to the logistics module.

Gap statement. Collectively, the literature confirms that linear MILP models are both accurate and computationally efficient for PV–CSP–H_2 hybrids; however, no prior study has examined simultaneous diesel *and* HFO displacement for a Middle-East mining operation. Filling this gap constitutes the principal contribution of the present study.

3 Methodology

3.1 Al Jalamid site context

Ma'aden's Al Jalamid phosphate operation in northern Saudi Arabia is an off-grid mine–processing complex. Electricity is presently supplied by a diesel-fuelled turbine plant, while heavy fuel oil (HFO) is trucked from Ras Al Khair and fired in the concentrate dryer. This configuration is operationally robust but carbon- and logistics-intensive. We investigate a behind-the-fence hybrid generation complex—concentrating solar power (CSP) with thermal energy storage (TES), utility-scale photovoltaics (PV), a lithium-ion battery energy storage system (BESS), and a proton-exchange-membrane (PEM) electrolyser—to fully decarbonise power and process heat services at the site.

3.2 Description of proposed system

The proposed system has all subsystems connect to a common $33\,\mathrm{kV}$ collector bus (AC). The solar panels - PV delivers low-cost daytime power; the CSP tower with molten-salt TES provides night-time and cloudy-period dispatchability without multi-hour round-trip losses; the BESS performs ramp-rate control and short-duration shifting; and the PEM converts surplus electricity into H_2 to displace HFO in the dryer burners. The topology mirrors utility-scale CSP–PV–battery hybrids in the literature (e.g. Hamilton et al., 2020), with the addition of on-site hydrogen production and an *explicit* materials balance linking H_2 to avoided HFO purchase and trucking.

Heliostat field The heliostat field comprises an array of dual-axis tracking mirrors that concentrate direct normal irradiance (DNI) onto the central receiver atop the CSP tower. Each

heliostat is individually oriented to maximise reflected flux on the receiver aperture throughout the day, compensating for solar position changes. Optical performance is characterised by mirror reflectivity, tracking accuracy, and cosine losses, while thermal performance accounts for atmospheric attenuation and spillage. In the MILP formulation, the field is parameterised by total reflective area (m^2), with hourly thermal energy capture calculated as the product of available DNI, field area, and a constant optical–thermal–cycle efficiency factor. This output is split between direct turbine feed and charging of the molten-salt thermal energy storage (TES), with the allocation optimised on an hourly basis.

Concentrating Solar Power tower - (CSP) + Thermal Energy Storage - (TES) In the molten-salt tower configuration, the heliostat field concentrates direct normal irradiance (DNI) onto a cavity receiver mounted atop a central tower. The receiver transfers the concentrated solar flux to circulating molten nitrate salt, heating it from a cold-tank temperature of approximately 290 to a hot-tank setpoint near 565. The heated salt is stored in a two-tank thermal energy storage (TES) system, enabling decoupling of solar collection from power generation. When electricity is required, hot salt is routed through a steam generator to raise superheated steam for a Rankine-cycle turbine, after which the cooled salt is returned to the cold tank for reheating. In the MILP formulation, TES capacity is expressed in turbine-hours and modelled in *electric-equivalent* kWh, preserving linearity in dispatch decisions while capturing the key temporal shifting capability of the thermal store.

Steam turbine generator. The Rankine-cycle steam turbine converts thermal energy from the molten-salt TES or directly from the solar receiver into mechanical rotation and then into electricity via an AC generator. Steam conditions are maintained at approximately 540 and 140 bar to optimise cycle efficiency and match commercially available turbine designs. The MILP formulation models the turbine as a dispatchable generation unit with a fixed nameplate capacity, expressed in kW_e, and constrains hourly output to be less than or equal to this rating. Thermal-to-electric conversion efficiency is represented as a constant factor, and auxiliary loads (parasitic consumption) are accounted for at the block level. The turbine provides firm baseload output when supplied from the TES and responds to intra-day fluctuations in thermal input from the CSP field.

Photovoltaic field - (PV) The photovoltaic (PV) subsystem consists of fixed-tilt or single-axis tracking (1P) module strings connected to central inverters. The layout is optimised to maximise plane-of-array irradiance capture while balancing land-use efficiency and cabling losses. A constant DC–AC conversion efficiency factor is applied in the MILP to represent inverter and balance-of-system (BOS) losses. The generated AC power can be routed to meet the instantaneous mine load, charge the battery energy storage system (BESS), supply the proton-exchange-membrane (PEM) electrolyser for hydrogen production, or—if economically favourable—exported to the grid. As the site is off-grid, the price is set to zero for this option, so that it is not incentivized in the economical balance. Curtailment is permitted when genera-

tion exceeds the combined instantaneous demand and storage charging capability, preserving operational realism in the optimisation.

Battery energy storage system - (BESS) The battery energy storage system (BESS) is implemented as a containerised lithium-iron-phosphate (LFP) installation, providing short- to medium-duration storage for smoothing photovoltaic (PV) output variability and shifting intra-day surplus generation to evening and night-time demand periods. In the MILP formulation, the BESS is modelled on the AC side, with separate charge and discharge variables and fixed one-way efficiencies for each direction, such that the round-trip efficiency is given by $\eta_{\text{rt}} = \eta_c \eta_d$. Operational limits include minimum and maximum state-of-charge (SOC) boundaries, as well as rated charge and discharge power capacities. The system primarily supports ramp-rate control, peak shaving, and firming of renewable generation to improve the reliability of supply to both the mining load and the electrolyser.

Proton-exchange-membrane electrolyser - (PEM) . The proton-exchange-membrane (PEM) electrolyser subsystem comprises modular stacks equipped with IGBT rectifiers, deionised water polishing, and control systems interfaced to the $33\,\text{kV}$ AC collector bus. The stacks convert electricity into low-pressure hydrogen gas, which is subsequently dried, compressed, and stored in above-ground bullet tanks for process use. In the MILP formulation, the electrolyser is represented with a fixed nameplate capacity and constant conversion efficiency, with the model enforcing an hourly hydrogen production requirement. Any shortfall relative to the target is captured through an unmet-demand variable, expressed in energy-equivalent terms, and penalised in the cost function. Produced H_2 displaces heavy fuel oil (HFO) in the beneficiation dryer at a substitution factor $\kappa_{\text{HFO}/\text{H2}}$ [kg/kg], thereby reducing HFO purchase costs and eliminating the need for long-haul tanker transport from coastal refineries.

3.3 MILP formulation

We adopt a lexicographic, two-pass mixed-integer linear program (MILP) inspired by Hamilton et al. (2020): Pass 1 minimises unmet *site* load; Pass 2 fixes that minimum and minimises net annual cost. In contrast to Hamilton et al. (2020), operational binaries are removed (purely continuous hourly dispatch), while integer variables determine the final sizes of each subsystem.

Service priorities. The optimiser first secures the critical *site* electricity each hour and only then allocates any remaining energy to H_2 generation. This “site□first” priority is enforced by a two□pass (lexicographic) objective (Section **??**).

3.4 Decision Variables

Let $t \in \mathcal{T} = \{1, \ldots, T\}$ index the hourly time steps over the optimisation horizon, where T typically corresponds to the total number of hours in a full year (e.g., $T = 8760$ for non-leap years). All balance equations, resource constraints, and dispatch decisions are enforced for each hour t individually, ensuring that generation, storage, demand, and operational limits are satisfied continuously throughout the year. This hourly resolution captures not only the intra-day and seasonal variability of plant performance and demand, but also the natural variability of the solar input over the year, providing a realistic representation of renewable generation profiles.

Integer sizing variables

$$n^{\mathsf{PV}},\ n^{\mathsf{Bat}},\ n^{\mathsf{EL}},\ n^{\mathsf{Turb}},\ n^{\mathsf{TES}},\ n^{\mathsf{Fld}}$$

Discrete capacity decisions defining the number of installed units of each subsystem: PV array (PV), battery (Bat), PEM electrolyser (EL), CSP steam turbine (Turb), thermal energy storage inventory (TES), and heliostat field aperture (Fld). These variables are the main levers of the sizing optimisation and are fixed across all time steps.

Hourly power flow variables

$$\begin{aligned}
&p_t^{\mathsf{PV}\to L},\ p_t^{\mathsf{PV}\to B},\ p_t^{\mathsf{PV}\to X},\ p_t^{\mathsf{PV}\to E}\\
&p_t^{\mathsf{F}\to T},\ p_t^{\mathsf{F}\to S},\ p_t^{\mathsf{S}\to T},\ y_t^{\mathsf{Turb}}\\
&p_t^{\mathsf{T}\to L},\ p_t^{\mathsf{T}\to B},\ p_t^{\mathsf{T}\to X},\ p_t^{\mathsf{T}\to E}\\
&p_t^{\mathsf{B}\to L},\ p_t^{\mathsf{B}\to E},\ e_t^{\mathsf{EL}}
\end{aligned}$$

These continuous variables represent the instantaneous AC (or electric-equivalent) power transfers between subsystems: - $p_t^{\mathsf{PV}\to L}$: PV power to site load; - $p_t^{\mathsf{PV}\to B}$: PV charging the battery; - $p_t^{\mathsf{PV}\to X}$: PV exported to grid; - $p_t^{\mathsf{PV}\to E}$: PV feeding the electrolyser; - $p_t^{\mathsf{F}\to T}$: CSP field thermal output sent directly to the turbine; - $p_t^{\mathsf{F}\to S}$: CSP field thermal energy stored in TES; - $p_t^{\mathsf{S}\to T}$: TES discharge to turbine; - y_t^{Turb}: gross turbine electric output; - $p_t^{\mathsf{T}\to L}, p_t^{\mathsf{T}\to B}, p_t^{\mathsf{T}\to X}, p_t^{\mathsf{T}\to E}$: turbine electricity routed respectively to load, BESS, export, or electrolyser; - $p_t^{\mathsf{B}\to L}, p_t^{\mathsf{B}\to E}$: battery discharge to load or electrolyser; - e_t^{EL}: total electric input to the electrolyser, summed from PV, CSP and battery sources.

These flows are constrained by subsystem availability, capacity limits, and efficiency factors, allowing the optimiser to determine the most economical routing each hour.

State-of-charge variables

$$E_t^{\mathsf{Bat}}, \quad E_t^{\mathsf{TES}}$$

Energy stored in the BESS (E_t^{Bat}, in kWh) and TES (E_t^{TES}, in electric-equivalent kWh$_e$) at the end of hour t. These evolve according to charge/discharge balance equations with round-trip

efficiency losses. Both are cyclic over the year to avoid end-of-horizon artefacts.

Unserved demand variables

$$u_t^{\text{Site}}, \quad u_t^{\text{H2}}$$

Slack variables capturing shortfalls in meeting the hourly critical site load (u_t^{Site}) and hydrogen demand (u_t^{H2}, expressed in electric-equivalent energy). These terms are penalised in the objective function — strictly in Pass 1 for site load and optionally for hydrogen depending on the scenario — ensuring reliability targets are respected before cost optimisation.

In all cases, the notation $(X \to Y)$ indicates an instantaneous power flow from subsystem X to subsystem Y. This consistent naming scheme makes it easier to trace the optimiser's routing decisions through the network each hour.

Integer sizing variables — these determine the discrete number of installed units for each asset class:

$$n^{\text{PV}},\ n^{\text{Bat}},\ n^{\text{EL}},\ n^{\text{Turb}},\ n^{\text{TES}},\ n^{\text{Fld}},$$

where PV = photovoltaic array, Bat = battery energy storage system, EL = PEM electrolyser, Turb = CSP steam turbine block, TES = thermal energy storage inventory, and Fld = CSP heliostat field.

Hourly operational decision variables — all are non-negative unless otherwise indicated:

$$\underbrace{p_t^{\text{PV}\to L}}_{\text{PV power to site load}}, \quad \underbrace{p_t^{\text{PV}\to B}}_{\text{PV power to BESS charge}}, \quad \underbrace{p_t^{\text{PV}\to X}}_{\text{PV power exported to grid}}, \quad \underbrace{p_t^{\text{PV}\to E}}_{\text{PV power to electrolyser}},$$

$$\underbrace{p_t^{\text{F}\to T}}_{\text{CSP field thermal output to turbine}}, \quad \underbrace{p_t^{\text{F}\to S}}_{\text{CSP field thermal charge to TES}}, \quad \underbrace{p_t^{\text{S}\to T}}_{\text{TES discharge to turbine}}, \quad \underbrace{y_t^{\text{Turb}}}_{\text{CSP turbine electric output}},$$

$$\underbrace{p_t^{\text{T}\to L}}_{\text{Turbine electric output to load}}, \quad \underbrace{p_t^{\text{T}\to B}}_{\text{Turbine electric output to BESS}}, \quad \underbrace{p_t^{\text{T}\to X}}_{\text{Turbine electric output exported}}, \quad \underbrace{p_t^{\text{T}\to E}}_{\text{Turbine electric output to EL}},$$

$$\underbrace{E_t^{\text{Bat}}}_{\text{BESS state of charge (kWh)}}, \quad \underbrace{E_t^{\text{TES}}}_{\text{TES state of charge (kWh}_e\text{)}},$$

$$\underbrace{p_t^{\text{B}\to L}}_{\text{BESS discharge to load}}, \quad \underbrace{p_t^{\text{B}\to E}}_{\text{BESS discharge to EL}}, \quad \underbrace{e_t^{\text{EL}}}_{\text{Total electric input to EL}},$$

$$\underbrace{u_t^{\text{Site}}}_{\text{Unserved site load}}, \quad \underbrace{u_t^{\text{H2}}}_{\text{Unserved hydrogen demand (energy eq.)}}.$$

The notation $(X \to Y)$ indicates the instantaneous power flow from subsystem X to subsystem Y. States of charge (E_t^{Bat}, E_t^{TES}) evolve according to storage balance equations with efficiency

losses, and unmet demand variables (u_t^{Site}, u_t^{H2}) capture any supply shortfall that is penalised in the objective function.

Resource and conversion constraints.

$$\text{PV availability:} \quad p_t^{\text{PV}\to L} + p_t^{\text{PV}\to B} + p_t^{\text{PV}\to X} + p_t^{\text{PV}\to E} \;\le\; G_t^{\text{POA}}\,\eta_{\text{inv}}\,(n^{\text{PV}} P_{\text{kWp}}^{\text{PV}}) \tag{1}$$

$$\text{CSP field:} \quad p_t^{\text{F}\to T} + p_t^{\text{F}\to S} \;\le\; \text{DNI}_t\,(n^{\text{Fld}} A_{\text{fld}})\,\eta_{\text{opt}}\eta_{\text{th}}\eta_{\text{cyc}} \tag{2}$$

$$\text{Turbine:} \quad y_t^{\text{Turb}} \;=\; p_t^{\text{F}\to T} + p_t^{\text{S}\to T}, \qquad y_t^{\text{Turb}} \;\le\; n^{\text{Turb}} P_{\text{kW}_\text{e}}^{\text{Turb}} \tag{3}$$

Network splits and balances.

$$\text{Turbine split:} \quad p_t^{\text{T}\to L} + p_t^{\text{T}\to B} + p_t^{\text{T}\to X} + p_t^{\text{T}\to E} \;=\; y_t^{\text{Turb}} \tag{4}$$

$$\text{Site balance:} \quad p_t^{\text{PV}\to L} + p_t^{\text{T}\to L} + p_t^{\text{B}\to L} + u_t^{\text{Site}} \;=\; D_t^{\text{Site}} \tag{5}$$

$$\text{Electrolyser routing:} \quad e_t^{\text{EL}} \;=\; p_t^{\text{PV}\to E} + p_t^{\text{T}\to E} + p_t^{\text{B}\to E} \tag{6}$$

$$\text{H}_2\text{ service:} \quad e_t^{\text{EL}} + u_t^{\text{H2}} \;=\; D_t^{\text{H2}} \quad \text{(energy-equiv.)} \tag{7}$$

$$\text{Electrolyser cap:} \quad e_t^{\text{EL}} \;\le\; n^{\text{EL}} P_{\text{kW}}^{\text{EL}} \tag{8}$$

Cyclic storage dynamics. Let $\eta_c\eta_d = \eta_{\text{rt}}$, with $\eta_c = \eta_d = \sqrt{\eta_{\text{rt}}}$.

$$\text{BESS SOC:} \quad E_{t+1}^{\text{Bat}} \;=\; E_t^{\text{Bat}} + \eta_c\Big(p_t^{\text{PV}\to B} + p_t^{\text{T}\to B}\Big) - \frac{1}{\eta_d}\Big(p_t^{\text{B}\to L} + p_t^{\text{B}\to E}\Big) \tag{9}$$

$$E_{\text{min}} \le E_t^{\text{Bat}} \le E_{\text{max}}, \qquad p_t^{\text{B}\to L} + p_t^{\text{B}\to E} \le n^{\text{Bat}} P_{\text{max}}^{\text{Bat}} \tag{10}$$

$$\text{TES SOC:} \quad E_{t+1}^{\text{TES}} \;=\; E_t^{\text{TES}} + p_t^{\text{F}\to S} - p_t^{\text{S}\to T}, \qquad E_t^{\text{TES}} \le n^{\text{TES}} E_{\text{kWh}}^{\text{TES}} \tag{11}$$

Cyclic boundary conditions close the year: $E_{T+1}^{\text{Bat}} = E_1^{\text{Bat}}$, $E_{T+1}^{\text{TES}} = E_1^{\text{TES}}$.

Pass 1 objective (site-first).

$$\min \sum_{t\in\mathcal{T}} u_t^{\text{Site}} \quad \text{s.t. (1)–(11) and bounds.} \tag{12}$$

Let $U^\star = \sum_t u_t^{\text{Site}}$ be the attained minimum; in Pass 2 we add $\sum_t u_t^{\text{Site}} = U^\star$ as an equality.

Pass 2 objective (net annual cost). The cost functional reproduces the cost function of replacing the current set-up, or complementing it, with the following component:

$$\min \quad \underbrace{r_c\, C_{\text{CAPEX}}(n)}_{\text{yearly financing cost of CAPEX}} + \underbrace{C_{\text{FOM}}(n)}_{\text{Opex O\&M}} + \underbrace{c_w \sum_t e_t^{\text{EL}}}_{\text{water for H}_2} + \underbrace{c_u \sum_t (u_t^{\text{Site}} + u_t^{\text{H2}})}_{\text{unserved penalty}} - \underbrace{(R_{\text{HFO}} + R_{\text{truck}} + R_{\text{CO2}} + R_{\text{siteload}})}_{\text{credits/revenues}}$$

with

$$
\begin{aligned}
C_{\text{CAPEX}} &= n^{\text{PV}} P^{\text{PV}}_{\text{kWp}} c^{\text{PV}} + n^{\text{Bat}} E^{\text{Bat}}_{\text{kWh}} c^{\text{Bat}} + n^{\text{EL}} P^{\text{EL}}_{\text{kW}} c^{\text{EL}} \\
&\quad + n^{\text{Turb}} P^{\text{Turb}}_{\text{kW}_\text{e}} c^{\text{Turb}} + n^{\text{TES}} E^{\text{TES}}_{\text{kWh}} c^{\text{TES}} + n^{\text{Fld}} A_{\text{fld}} c^{\text{Fld}}, \\
C_{\text{FOM}} &= n^{\text{PV}} P^{\text{PV}}_{\text{kWp}} o^{\text{PV}} + n^{\text{Bat}} E^{\text{Bat}}_{\text{kWh}} o^{\text{Bat}} + n^{\text{EL}} P^{\text{EL}}_{\text{kW}} o^{\text{EL}} + n^{\text{Turb}} P^{\text{Turb}}_{\text{kW}_\text{e}} o^{\text{Turb}}, \\
R_{\text{HFO}} &= \left(\kappa_{\text{HFO/H2}}\, \sigma_{\text{H2}} \sum_t e^{\text{EL}}_t\right) p_{\text{HFO}}, \qquad \sigma_{\text{H2}} = \frac{\eta_{\text{EL}}}{33.3}\ \ [\text{kg/kWh}], \\
R_{\text{truck}} &= \left(\kappa_{\text{HFO/H2}}\, \sigma_{\text{H2}} \sum_t e^{\text{EL}}_t\right) \frac{d_{\text{haul}}}{Q_{\text{truck}}}\, p_{\text{haul}} \quad \text{(avoided trips)}, \\
R_{\text{CO2}} &= \Big(\underbrace{\theta^{\text{comb}}_{\text{CO2}} + \theta^{\text{road}}_{\text{CO2}}}_{\text{scope 1 + freight}}\Big) \left(\kappa_{\text{HFO/H2}}\, \sigma_{\text{H2}} \sum_t e^{\text{EL}}_t\right) p_{\text{CO2}} \\
&\quad + \theta^{\text{CH4}} p_{\text{CH4}} + \theta^{\text{N2O}} p_{\text{N2O}} \quad \text{(same factorisation by displaced HFO mass)}, \\
R_{\text{siteload}} &= p_{\text{kwh}} \sum_t \left(p^{\text{PV}\to X}_t + p^{\text{T}\to X}_t\right).
\end{aligned}
$$

All unit costs/parameters correspond to fields in your `econ` and `unit` structs.

3.5 Solution approach and dispatch logic

We solve Pass 1 and Pass 2 with MATLAB's `intlinprog`. Only the sizing variables $\{n^{\cdot}\}$ are integer; all hourly dispatch variables are continuous. Battery and TES are cyclic over the year, which steers the MILP away from pathological end effects. The electrolyser meets the hourly H_2 target if economic (Eq. 7); otherwise $u^{\text{H2}}_t > 0$ is penalised. The optimiser routes PV first to the mine (Eq. 5), then to the PEM and BESS if beneficial; CSP provides evening and night service via Eqs. (2)–(4). This policy mirrors the hybrid dispatch logic shown for utility-scale CSP–PV–battery systems (Hamilton et al., 2020, pp. 341–349).

Inputs (driver `run_milp_milp_v2_lex.m`). The driver (i) aligns hourly timestamps across irradiance (G_{POA} or GHI), DNI, site load (diesel proxy) and H_2 demand; (ii) loads techno-economics (`unit`, `econ`); and (iii) optionally truncates to a smoke-test horizon. Units are normalised to kWh (AC) per hour and kg of H_2 via $\sigma_{\text{H2}} = \eta_{\text{EL}}/33.3$.

The driver aligns hourly irradiance (G_{POA}), DNI, site load and H_2 demand, then solves Pass 1 & Pass 2 with `intlinprog`; outputs are written to `Hourly`, `Monthly`, `Summary`, `CostBreakdown`, `Emissions`, `Assumptions` sheets for auditability.

Below it is a description of the single Excel workbook and its sheets that support the auditability of the model, the results were also validate with estimated costs for such investment as shown in Section H :

- **Hourly:** time series of irradiance, DNI, per-hour PV and CSP potentials, turbine output and splits, TES/BESS SOC, electrolyser energy and H_2 production, served/unserved energy and grid export. Columns 'Elec_from_PV/CSP/Batt' show exact attributions to the PEM.

- **Monthly:** calendar sums of 'PV_kWh', 'CSP_Field_kWh_e', 'H2_demand_total_kg', 'H2_prod_total_kg', and 'Site_Load_kWh'.
- **Summary:** annual KPIs (total H_2 [kg], displaced HFO [kg], export [kWh], areas, total CAPEX and annualised CAPEX, fixed OPEX, water/trucking costs, avoided-fuel revenue, export revenue, net cost, and emissions avoided).
- **CostBreakdown:** the same totals disaggregated by subsystem (PV, PEM, BESS, CSP turbine, TES, heliostat field), plus derived size metrics (MWp, MW, MWh, m^2).
- **Emissions:** annual avoided combustion CO_2, road-freight CO_2, avoided CH_4 and N_2O.
- **Assumptions:** a flat dump of `econ` and `unit` for auditability.

3.6 How the suggested approach relates to the literature and mirrors the real process

The linear, network-flow structure and TES□to-power abstraction follow the hybrid dispatch formulations in Hamilton et al. (2020), who show that PV–CSP–battery hybrids materially improve capacity factors and economics compared with CSP-only plants (their Fig. 11 and Table 7). Our contributions are (i) an off-grid, site-first lexicographic objective; (ii) an explicit PEM module that couples electricity to a process-fuel ledger; and (iii) the cost/credit structure for avoided HFO, long-haul freight and life-cycle GHG accounting.

Site Load Electric service. Crushing, grinding, flotation and utilities run 24/7; the MILP's site stream D_t^{Site} represents that demand. Turbine output and PV are routed to the site first; BESS smooths ramps and short deficits.

Thermal service via H_2. The dryer's fuel ledger is coupled to electrolyser production through a fixed displacement factor ($\kappa_{\text{HFO/H2}}$ kg/kg). The optimisation weighs H_2 output (water use, CAPEX) against avoided HFO purchases, avoided long□haul trucking and monetised emissions.

Why lexicographic. A single weighted sum can hide corner cases where the solver prefers cheap H_2 at the expense of short electric outages. The two□pass scheme bans that: Pass 1 finds the minimum unserved site energy; Pass 2 only optimises cost among solutions that meet that minimum. In effect, *reliability is a hard constraint, not a soft preference*.

3.7 The CVaR Extension

For risk analysis, a CVaR (Conditional Value-at-Risk)(or VaR) variant replaces the single□year resource with a 10□year irradiance ensemble and minimises expected cost plus a CVaR term at a chosen confidence level (e.g., 95%), preserving the same network and sizing structure. This yields designs that keep the site load served across adverse years while quantifying the premium for resilience.

This extension replaces the single-year resource record with a multi-year irradiance ensemble (S scenarios, each of length T hours) and minimises the sum of expected cost and a risk term proportional to the tail loss beyond the α-quantile. This produces designs that are robust to inter-annual solar variability, at theriables $x_{t,s}$ are scenario-indexed (t, s). Two cases were implement, the site load only and Site + H2. These CVaR variants preserve the same network-flow constraints and integer sizing variables as the one-year MILP in Section 3.3. The key changes are:

- All hourly operational variables $x_{t,s}$ are scenario-indexed (t, s).
- The Pass 1 objective minimises the sum of unserved *site* load over all scenarios.
- Pass 2 fixes this minimum and minimises:

$$\min \ \mathbb{E}_s \left[\mathsf{Cost}(n, x_{\cdot,s})\right] \ + \ \lambda \cdot \mathsf{CVaR}_\alpha(\mathsf{Loss}_s) \tag{13}$$

  where λ is the risk-aversion weight, α the confidence level, and Loss_s the monetised unserved energy in scenario s.

Site-only CVaR. In this formulation, the optimisation ensures only that the *electrical* site load D_t^{Site} is met across all scenarios. Hydrogen production is *not* modelled as a constraint: any H_2 reported is a post-hoc calculation from surplus (export/dump) energy and does not influence sizing.

$$\text{Pass 1:} \qquad \min \quad \sum_{s=1}^{S} \sum_{t=1}^{T} u_{t,s}^{\mathsf{Site}} \tag{14}$$

$$\text{Pass 2:} \qquad \min \quad \sum_{s=1}^{S} p_s \, \mathsf{Cost}_s + \lambda \left[z + \frac{1}{1-\alpha} \sum_{s=1}^{S} p_s \, \epsilon_s \right] \tag{15}$$

$$\text{s.t.} \quad \mathsf{Loss}_s - z \le \epsilon_s, \quad \epsilon_s \ge 0 \tag{16}$$

Here, $\mathsf{Loss}_s = c_u \sum_t u_{t,s}^{\mathsf{Site}}$, with c_u the penalty for unmet site load. Only PV, CSP (field, TES, turbine) and BESS units appear in the design vector n.

Site + Hydrogen CVaR. This variant enforces both *site load* and *hydrogen demand* each hour:

$$e_{t,s}^{\mathsf{EL}} + u_{t,s}^{\mathsf{H2}} = D_t^{\mathsf{H2}}, \quad \forall t, s \tag{17}$$

$$p_{t,s}^{\mathsf{PV}\to L} + p_{t,s}^{\mathsf{T}\to L} + p_{t,s}^{\mathsf{B}\to L} + u_{t,s}^{\mathsf{Site}} = D_t^{\mathsf{Site}} \tag{18}$$

The Pass 1 objective remains to minimise *site* unmet load, but in Pass 2 the cost function includes penalties for both unserved site electricity and unserved hydrogen (energy-equivalent):

$$\mathsf{Loss}_s = c_u^{\mathsf{Site}} \sum_t u_{t,s}^{\mathsf{Site}} + c_u^{\mathsf{H2}} \sum_t u_{t,s}^{\mathsf{H2}}. \tag{19}$$

The design vector n now includes electrolyser units n^{EL}, increasing coupling between PV/CSP/BESS sizing and the H_2 production block.

Key differences to one-year MILP.

1. **Scenario indexing:** The single-year MILP uses T hourly steps; CVaR variants use $T \times S$ steps and scenario probabilities p_s.
2. **Risk term:** Objective (13) adds a CVaR penalty, absent in the one-year case.
3. **Site-only vs. Site + Hydrogen:** The former ignores hydrogen in sizing; the latter co-optimises both site and H_2 service.

This separation allows estimating the minimal incremental CAPEX required to ensure site resilience, and the additional premium to guarantee full hydrogen production under adverse solar years.

4 Input Data

This section documents the datasets, transformations, and parameters used by the optimization model. The optimization is done over every hour of a full year, in order to achieve that all time–series are aligned on a single master timeline `TimeUTC` (UTC timezone for Saudi Arabia). Most of the optimization is done for considering a single–year and it uses the calendar year 2022. The CVaR analysis uses a Multi–year scenario analyses that cover the years from 2013–2022 (ten complete years). In the next subsection sources and the example of the data set are present, the first ones are the ones necessary to input into the PV and CSP, then it is presented the operational data provided by Al Jalamid site, and lastly the data recompiled from benchmarked implementations and reports that outlines the operational and economic performance of the simulated equipment.

4.1 NASA POWER irradiance datasets (PV & CSP)

These data sets are relevant as input for the Energy that is generated by the PV and the CSP. Therefore they were retrieved as a plane-of-array proxies via global horizontal irradiance (GHI) and direct normal irradiance (DNI) from NASA POWER (community: `RE`) at the Al Jalamid site coordinates (e.g., $31.200\,°$N, $39.850\,°$E). NASA provides hourly means in $\mathrm{W\,m^{-2}}$; that was converted to hourly energy densities in $\mathrm{kWh\,m^{-2}\,h^{-1}}$ by dividing by 1000.

Year 2022 (single-year).

- `irradiance_hourly.mat`: `TimeUTC` (8760 rows), `GHI_kWhm2`.
- `dni_hourly.mat`: `TimeUTC` (aligned), `DNI_kWhm2`.

Years 2013–2022 (ten-year scenarios).

- `irradiance_hourly_2013-2022.mat`: concatenated hourly `GHI_kWhm2` with `TimeUTC`.
- A union-join merge the GHI and DNI timelines, fill $\leq$3-hour gaps by linear interpolation (endpoints by nearest), and drop 29-Feb (from leap years in the time horizon) rows so each year is 8760 h.

Acquisition & alignment. Hourly data are fetched year-by-year using the POWER endpoint for `ALLSKY_SFC_SW_DWN` (GHI) and `ALLSKY_SFC_SW_DNI` (DNI). Responses may be requested in `UTC` or `LST`, but LST is the one used in Saudi Arabia; all series are re-keyed to the master `TimeUTC` axis for modelling.

Table 6: NASA files and variables.

File	Vars	Units	Hours	Notes
`irradiance_hourly.mat`	`TimeUTC`, `GHI_kWhm2`	kWh m^{-2} h^{-1}	8760	Year 2022
`dni_hourly.mat`	`TimeUTC`, `DNI_kWhm2`	kWh m^{-2} h^{-1}	8760	Year 2022
`irradiance_hourly_2013-2022.mat`	`TimeUTC`, `GHI_kWhm2`	kWh m^{-2} h^{-1}	10×8760	2013–2022, no leap-day
`dni_hourly_10Y.mat`	`TimeUTC`, `DNI_kWhm2`	kWh m^{-2} h^{-1}	10×8760	2013–2022, aligned to GHI

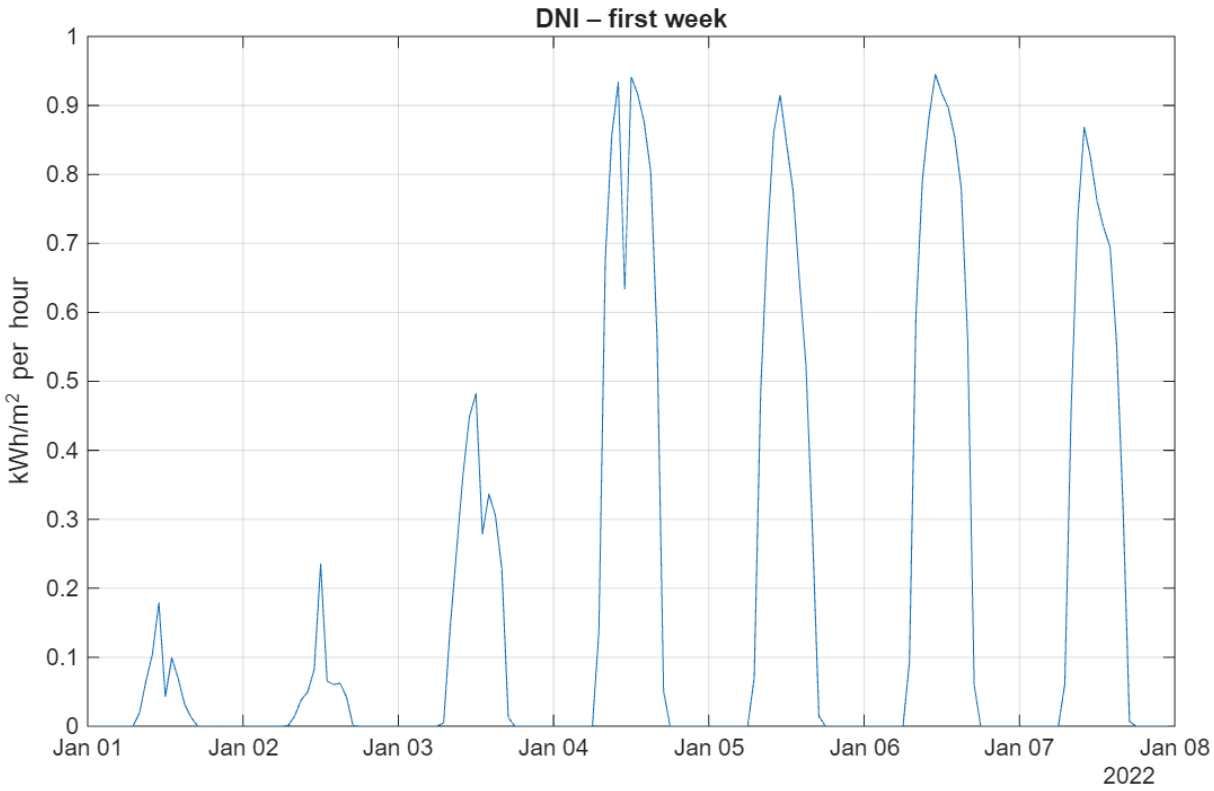

Figure 2: Illustrative DNI dynamics for first week of 2022 (hourly).

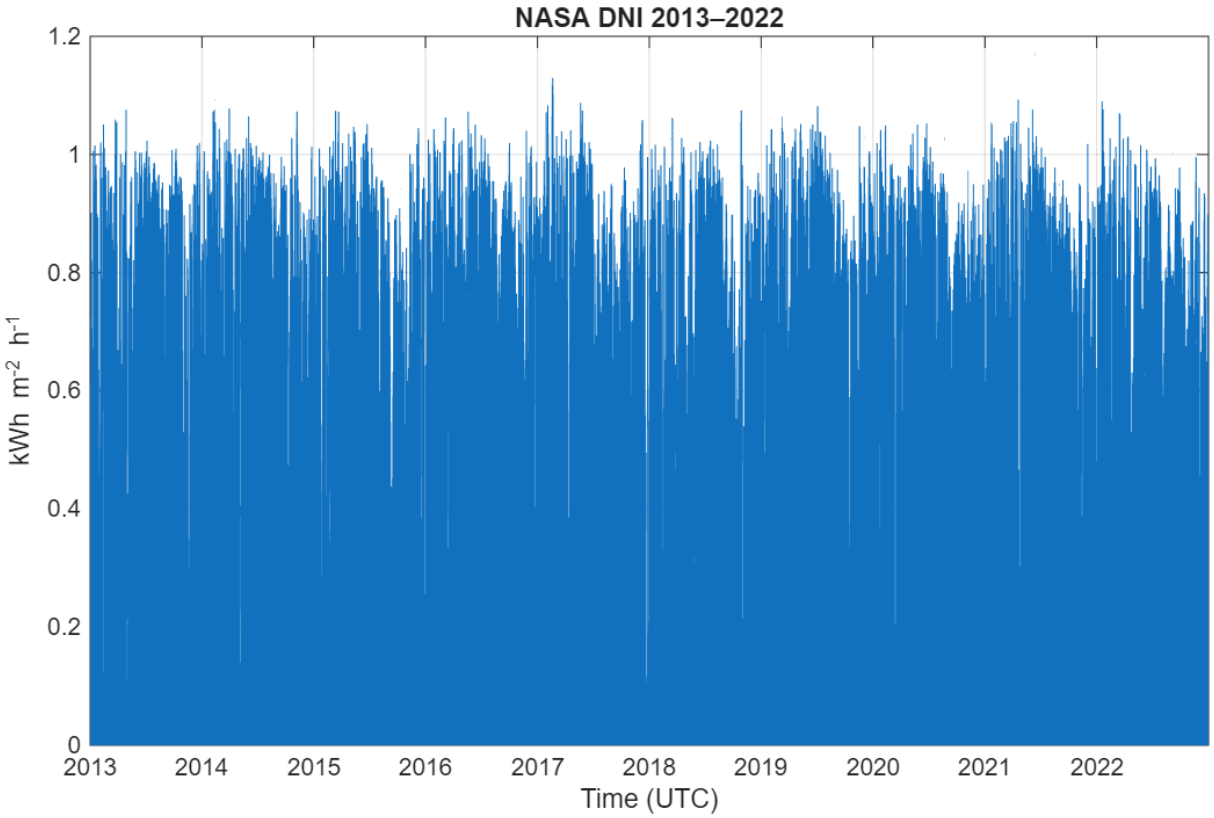

Figure 3: Multi-year distributions of irradiance (2013–2022).

4.2 Ma'aden operational data: HFO consumption and Electricity generated by the site

Monthly HFO consumed. The monthly heavy fuel oil (HFO) tonnages consumed in 2022 was provided and it was read from Excel and converted to hydrogen needed using an LHV-based factor (HFO $\approx 40\,\mathrm{MJ/kg}$, $H_2 \approx 120\,\mathrm{MJ/kg}$), i.e.,

$$H_2 \text{ t/month} \;=\; 0.333 \times \text{HFO t/month}.$$

Two profiles were created:

1. **As is (monthly-even)**: Considering the actual monthly consumption the Demand of H_2 was spread evenly across all hours of that month.
2. **Irradiance-shaped (optional)**: the annual H_2 total is distributed hourly in proportion to the normalised CSP field irradiance (DNI-based), preserving the same annual sum.

Example of the used data:

Table 7: Sample months: As is — `Monthly_H2_100_need.xlsx`.

Month	Name	HFO (t)	H_2 (t)
1	January	5,853,995	1,949,380
4	April	6,168,933	2,054,255
7	July	5,512,686	1,835,724
10	October	3,919,811	1,305,297

Table 8: Sample months: Irradiance-shaped — `Monthly_H2_100_level.xlsx`.

Month	Name	HFO (t)	H_2 (t)
1	January	4,847,788	1,614,313
4	April	4,174,164	1,389,996
7	July	7,792,222	2,594,810
10	October	4,667,796	1,554,376

Site generated electricity (kWh). The daily total electricity generated by the diesel powered turbines (kWh/day) are read from the provided Excel and split evenly across the 24 hours of each day, after aligning dates to `TimeUTC` and handling leap-year mismatches (drop 29-Feb as needed). Example (first 7 days, using the "Total kWh" column):

Table 9: Daily Energy (kWh) totals and implied hourly split (example, first 7 days).

Day	Total (kWh/day)	Hourly split (kWh/h)
1	441,000	18,375.00
2	436,000	18,166.67
3	459,000	19,125.00
4	446,000	18,583.33
5	448,900	18,704.17
6	446,000	18,583.33
7	462,400	19,266.67

4.3 Economic and unit parameters (`econ` and `unit`)

Tables 10 and 11 list the operational and economic parameters that describe each component of the proposed solution, in Appendix C and Appendix D are detailed the sources.

Table 10: Technology unit parameters (`unit`).

Item	Parameter	Value
PV	P_{kWp}	1 kWp per unit
	CAPEX	\$550 / kWp
	OPEX	\$12 / kWp·yr
	Inverter efficiency	0.97 (–)
	Area density	$6\,\text{m}^2$/kWp
BESS	Energy per unit	$250\,$kWh
	CAPEX	\$250 / kWh
	OPEX	\$7.5 / kWh·yr
	Round-trip efficiency	0.92 (–)
	Max charge / discharge	$250\,$kWh$/$h (AC)
	SOC bounds	10–95%
Electrolyser	Power per unit	$500\,$kW
	CAPEX	\$1,950 / kW
	OPEX	\$75 / kW·yr
	Efficiency (LHV)	0.70 (–)
CSP (turbine)	Unit size	$10\,$MW_e per unit
	CAPEX	\$1,500 / kW_e
	OPEX	\$65 / kW_e·yr
CSP (TES)	Storage unit	$50\,$MWh_e per unit
	Charge rate	Unit/8 h
	CAPEX	\$30 / kWh_e
CSP (field)	Aperture area	$1000\,\text{m}^2$ per unit
	Optics eff.	0.80 (–)
	Thermal eff.	0.55 (–)
	Cycle eff.	0.38 (–)
	CAPEX	\$200 / m^2

Table 11: Economic & environmental parameters (`econ`).

Item	Parameter	Value
Fuel substitution	kg HFO per kg H_2	3.0
	HFO price	\$0.40 / kg
Logistics	Truck capacity (HFO)	30.000 kg
	Transport distance	2400 km
	Trucking cost	\$2.0 / km
Emission factors	HFO CO_2/CH_4/N_2O	3.2327 / 0.0030 / 0.0072 kg/kg
Road freight EF	CO_2	2.68 kg / t·km
Water	Electrolysis req.	9 L / kg H_2
	Water price	\$4.0 / m^3
Electricity value	Excess energy proxy	\$0.20 / kWh
	Export price	\$0.00 / kWh
Carbon prices	CO_2/CH_4/N_2O	\$0.05 / \$0.54 / \$5.46 per kg
Finance	Annualised CAPEX rate	2%
Reliability	Unserved energy penalty	\$50 / kWh

5 Results and Discussion

This section synthesises the optimisation results and sensitivity analyses to highlight how carbon pricing, production planning and reliability constraints influence the hybrid PV–CSP–BESS–PEM design for Al Jalamid. Four deterministic scenarios were run: a *base* case with zero emission price, a *KAPSARC* case with an emissions price reflecting KAPSARC's \$150 $t_{CO_2}^{-1}$ outlook for 2030, and two *levelled* cases where phosphate production is scheduled to coincide with the solar resource (Level H_2 base and Level H_2 KAPSARC). Table 12 compares the key outcomes.

Table 12: Key metrics for deterministic scenarios (values rounded). $CAPEX_{ann.}$ denotes the annualised financing cost at 2%. Unserved energy and H_2 production are annual totals.

Scenario	Description	CAPEX (M USD)	$CAPEX_{ann.}$ (M USD yr^{-1})	Unserved energy (GWh yr^{-1})	H_2 prod. (kt yr^{-1})	Net cost (M USD yr^{-1})
Base (0 USD/kg)	No carbon price; least–cost dispatch.	246	4.92	944	1.31	-31.3
KAPSARC 2030	p_{CO_2} = *0.15* USD kg^{-1}; min-imises net cost.	1 305	26.1	53.9	20.0	-61.3
Level H_2 base	Production aligned with irra-diance; $p_{CO_2} = 0$.	246	4.92	944	1.31	-31.3
Level H_2 KAPSARC	Irradiance–aligned produc-tion; $p_{CO_2} = 0.15$ USD kg^{-1}.	1 225	24.5	99.9	19.1	-60.9

5.1 Deterministic scenarios

The *base* scenario invests only \$246 M in CAPEX to meet the minimum constraint of avoiding unmet critical load, but leaves the majority of the phosphate plant's electrical demand unmet. Approximately 944 GWh of unmet energy (about half of the site load) must continue to be supplied by diesel gensets, and only 1.31 kt of green hydrogen is produced. Even so, fuel displacement revenues exceed water and O&M costs, yielding a net cost of -31.3 M USD yr^{-1}.

Introducing a carbon price consistent with KAPSARC's 2030 outlook (\$0.15 kg^{-1}) shifts the optimum toward a very large plant: the *KAPSARC* scenario installs 520 MW_p PV, 370 MWh TES and a 10 MW CSP turbine, with a total CAPEX of \$1.305 B (annualised cost \$26.1 M). Unserved energy falls to 53.9 GWh and 20.0 kt of H_2 are produced. The net cost improves to -61.3 M USD yr^{-1} because avoided HFO and CO_2 credits offset the higher investment.

Aligning production with the solar resource (Level H_2 base) yields nearly identical results to the base case—because the carbon price is zero the optimiser still favours a small plant and accepts large unmet energy. When the KAPSARC price is applied under the levelled production plan, a slightly smaller investment (\$1.225 B) is sufficient because production is curtailed during low irradiance periods. This "smoothed" dispatch sacrifices a modest amount of H_2 output (19.1 kt vs. 20.0 kt) and leaves 99.9 GWh unmet, but still achieves a comparable net saving (-60.9 M).

5.2 Carbon-price sensitivity

Figures 4–5 plot the response of CAPEX, net cost, unserved energy and H_2 production when the shadow price of CO_2 is swept from 0 to 0.15 USD kg^{-1} for four design contexts: (i) base (no penalty for unmet demand), (ii) base with a high penalty on unmet demand, (iii) levelled production with no penalty, and (iv) levelled production with a penalty. The sensitivity curves were generated using the spreadsheet "CO_2 sweep results" contained in the supplementary files.

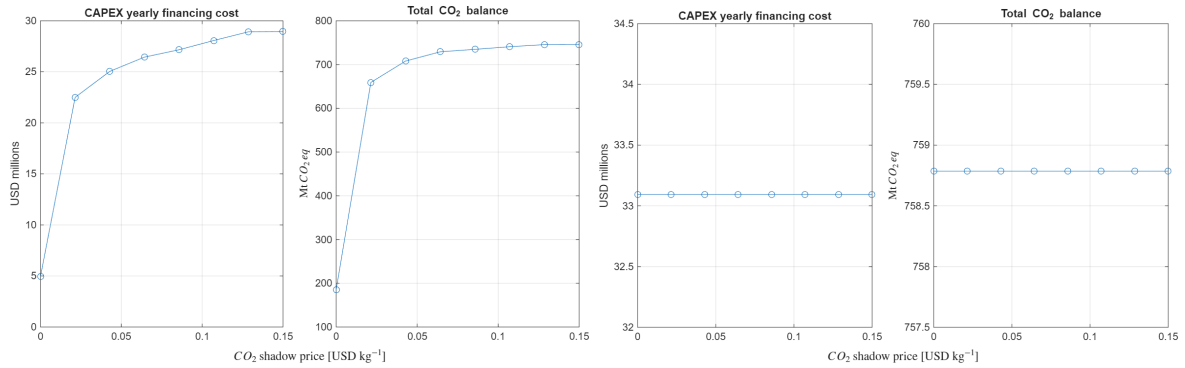

Figure 4: Carbon□price sensitivity for the base scenarios. Left: CAPEX growth and CO_2 balance without a reliability penalty. Right: results when unmet demand incurs a high penalty.

Without a penalty (left panel of Fig. 4), total CAPEX grows steeply from ≈250 M USD at zero price to ≈1.35 B USD at 0.05 USD kg^{-1}, after which it saturates. Net cost becomes more negative with price (largely due to avoided carbon emissions). Unserved energy collapses from $\sim 9.4 \times 10^5$ MWh to a few tens of thousands of MWh as the optimiser adds storage and CSP capacity. H_2 output increases from ∼1.4 kt to ∼20 kt. When a high penalty is applied to unmet demand (right panel), the optimiser immediately installs the full CSP–PV–BESS–PEM complement (CAPEX ≈1.65 B USD) even at zero carbon price; unserved energy is driven to zero and H_2 production fixed at ∼21.17 kt. Increasing the carbon price then only affects the net cost (via credit revenues).

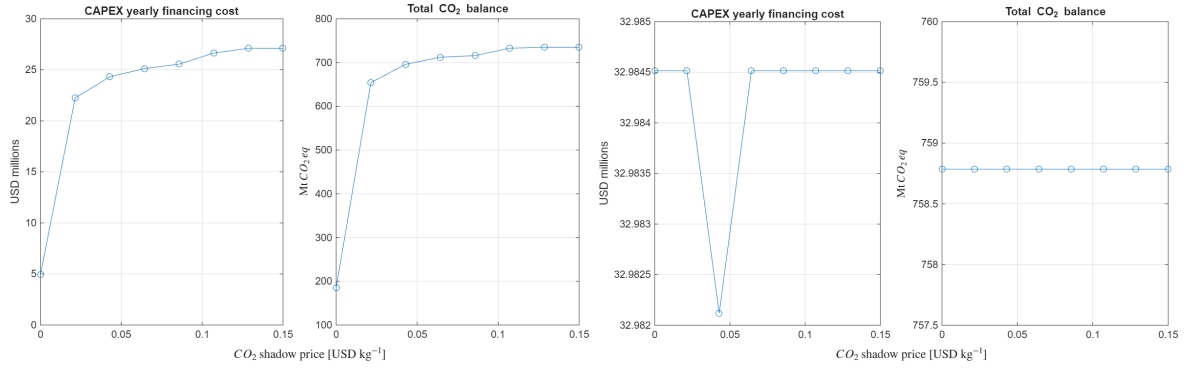

Figure 5: Carbon□price sensitivity for irradiance□levelled production. Left: no unmet□demand penalty. Right: full penalty for unmet demand.

Figure 5 shows analogous curves for the levelled production cases. Without penalty (left), the patterns are similar to the base case: CAPEX grows from ≈250 M USD to ≈1.35 B USD as the

carbon price rises; H_2 output rises to ≈20 kt and unserved energy falls sharply. With a penalty (right), the system again installs a large plant irrespective of the carbon price; CAPEX stays nearly constant ($1.65 B) and net cost decreases linearly with price.

5.3 Production scheduling and investment

The “levelised’’ runs underline the importance of matching production to the renewable resource. By aligning beneficiation and drying operations with high-irradiance hours, the Level H_2 KAPSARC design achieves a comparable emissions reduction to the fully sized KAPSARC plant but with approximately 6 % less CAPEX (1.23 B vs. 1.30 B). However, this comes at the cost of a larger unserved energy penalty and a modest reduction in H_2 output. In practice, the phosphate plant may be able to shift some operations but not fully curtail; thus the actual optimum is likely between these extremes.

5.4 Reliability and risk analysis

Finally, a conditional value-at-risk (CVaR) formulation was solved using ten years (2013–2022) of NASA irradiance data. In the *site-only* CVaR case, only the mining load is hedged; results were nearly identical to the base case because the optimiser could accept very large unmet hydrogen. In the *full-demand* CVaR case, both electricity and hydrogen demands were hedged at the 80th percentile; the resulting design matched the “full penalty’’ investment profile in Figs. 4–5, demonstrating that meeting demand under worst-year insolation requires sizing the plant to the same level as the deterministic full-penalty solution. Thus the CVaR results support the conclusion that avoiding curtailment of the diesel plant (unserved energy) dominates the optimal sizing decision.

In summary, increasing the CO_2 price strongly incentivises larger investments in PV, CSP and storage; adding penalties for unserved load or hedging irradiance risk forces investment to the upper end of the CAPEX range regardless of the carbon price. Aligning the production schedule with the solar resource can reduce the required CAPEX at high carbon prices, but this lever must be balanced against increased unmet load and lower H_2 output.

6 Data analysis and discussion

Workflow and scenarios. We solve a two-pass (lexicographic) MILP over an annual horizon: Pass 1 minimises unmet *critical* load (site reliability), Pass 2 fixes that minimum and then minimises the annualised net cost (CAPEX annuity, fixed O&M, fuel savings, water, trucking, carbon charges/credits, and unmet-energy penalties). Dispatch blocks (PV, CSP+TES, BESS, PEM) follow the linear hybrid formulation used in utility-scale studies of PV–CSP–storage hybrids, adapted here to include electrolyser and site-load constraints. The rolling-horizon solution (48 h with 24 h look-ahead) mirrors established practice for tractable annual runs. (cf. Hamilton et al., 2020). We analyse four scenario families: (i) *Base* (no CO_2 price); (ii) *KAPSARC-2030* expected CO_2 shadow price; (iii) *Levelised H_2* (production plan aligned to irradiance); and (iv) *Levelised H_2+Full Penalty* (no unmet demand permitted). Each family is then stressed over a CO_2 price sweep $p_{CO_2} \in [0, 0.15]$ USD kg^{-1}. Finally, we embed 10 years of hourly irradiance (2013–2022) in a risk-aware design using CVaR for two reliability scopes: *Site-only* and *Site+H_2*.

6.1 Headline metrics (fill from spreadsheets)

To keep the narrative compact in the main text, Table 13 concentrates the KPIs you'll cite throughout (pull values from the four Excel workbooks named in the text). Where a KPI is "per year", report it as an annual average over the simulated year.

Table 13: Headline KPIs by scenario (to be populated from the provided spreadsheets).

KPI	Base (no CO_2)	KAPSARC-2030	Levelised H_2	Levelised H_2+Full Penalty
Total CAPEX [USD m]				
CAPEX annuity [USD m y^{-1}]				
Net cost [USD m y^{-1}]				
Unserved energy [MWh y^{-1}]				
H_2 production [t y^{-1}]				
Total CO_2 balance [t y^{-1}]				

Populate from: *202508031551_H2_CSP_System_AllResults_MILP_lex_v2Selected result base scenario.xlsx*, *202508031636_..._Expected Price KAPSARC 2030.xlsx*, *202508041249_..._Level H2 base scenario.xlsx*, *202508041300_..._Level H2 Expected Price KAPSARC 2030.xlsx*.

6.2 Carbon-price sensitivity (Base)

Figure 6 (pair) and Figure **??** (panel grid) summarise how the base design responds as p_{CO_2} rises from 0 to 0.15 USD kg^{-1}. CAPEX annuity and total CAPEX increase and then plateau, unserved energy collapses rapidly towards zero, and H_2 output rises towards a ceiling; net cost trends downward (more negative) as credits/avoided emissions accrue. The CO_2 balance chart confirms monotonically improving emissions performance.

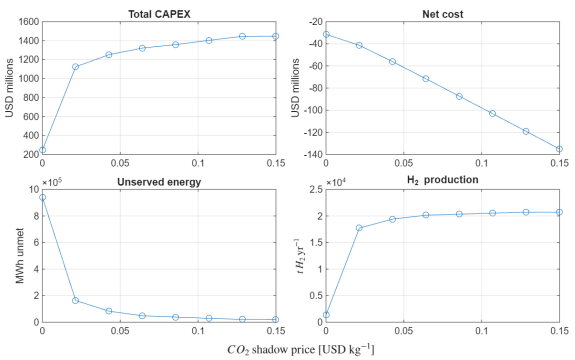

CAPEX yearly financing cost vs. p_{CO_2}.

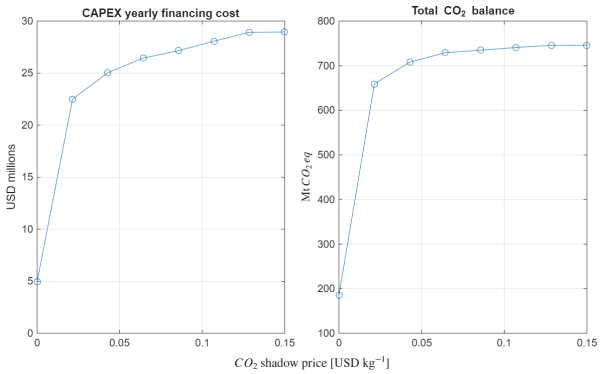

Total CO_2 balance vs. p_{CO_2}.

Figure 6: Carbon-price sensitivity—Base scenario (no unmet-demand penalty).

6.3 Adding a penalty for unmet demand

When unmet energy is fully penalised, the optimiser is forced to zero outages; capacity becomes the control knob while cost and credits adapt linearly with p_{CO_2}. In your runs this produces flat CAPEX/H_2/unserved-energy traces with a roughly linear net-cost decline.

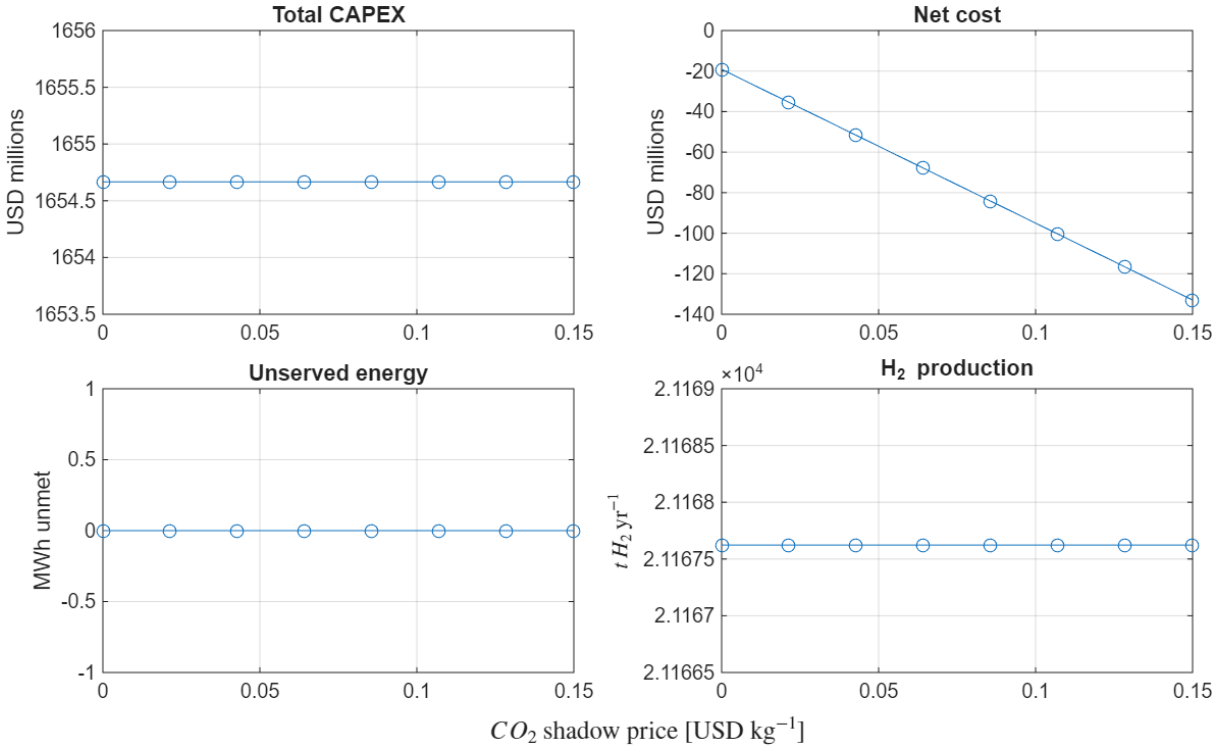

Figure 7: Penalty for unmet demand: Total CAPEX, net cost, unserved energy, and H_2 production vs. p_{CO_2}.

6.4 Levelised H_2 production plan

Shifting the production plan to follow irradiance (Levelised H_2) reduces PV curtailment and TES cycling, improving hydrogen yield per unit of CAPEX and pushing the unserved-energy curve

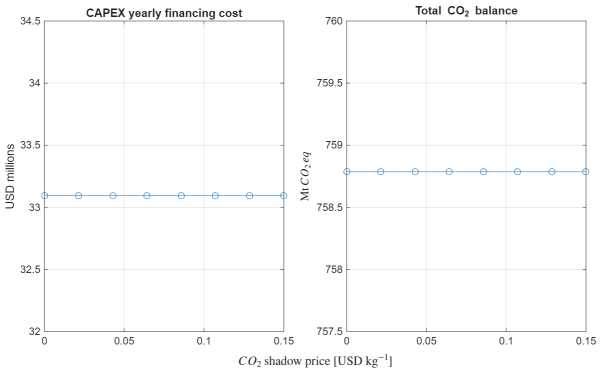

(CO_2 balance panel—include if available)

CAPEX yearly financing cost vs. p_{CO_2}.

Figure 8: Penalty for unmet demand: financing and (optionally) CO_2 balance.

down faster at low p_{CO_2}. As prices rise, CAPEX saturates and the system approaches a dispatch ceiling.

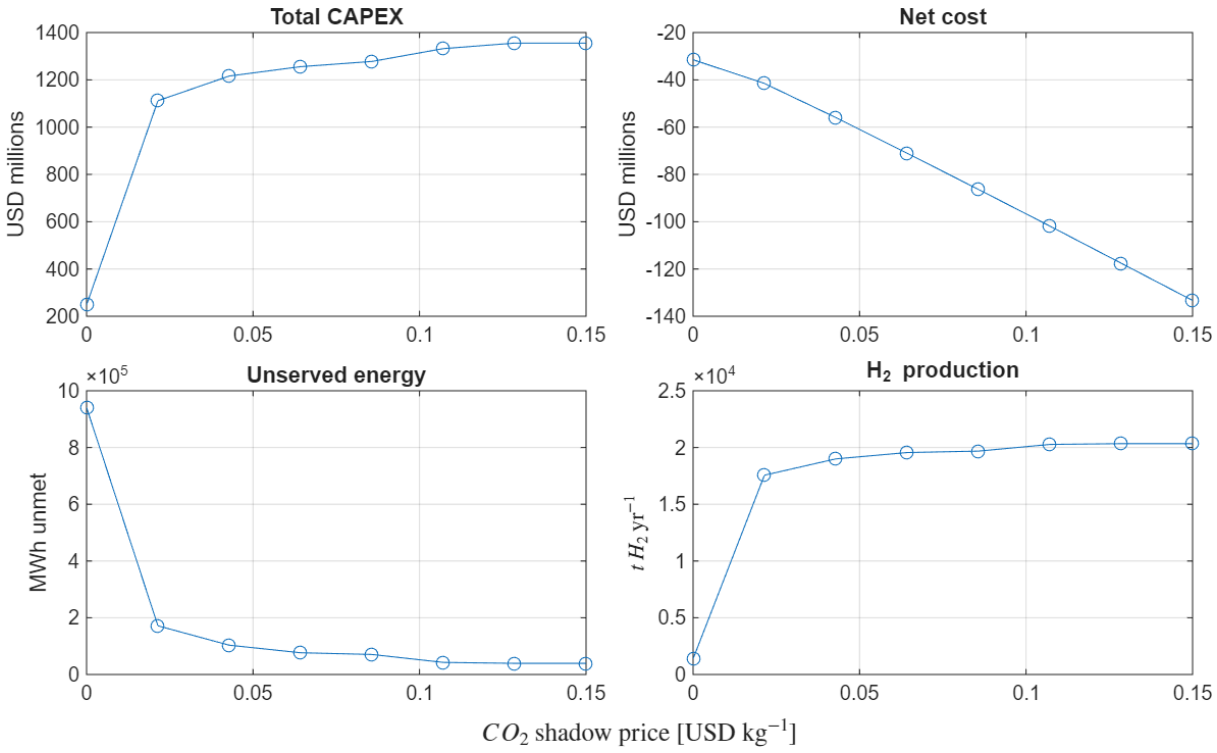

Figure 9: Levelised H_2: Total CAPEX, net cost, unserved energy, and H_2 production vs. p_{CO_2}.

6.5 Levelised H_2 with full penalty

With both a levelised production plan and a full reliability constraint, the optimiser settles on a capacity mix that eliminates unmet energy across the sweep; only net cost moves materially with p_{CO_2}, driven by emissions pricing/credits.

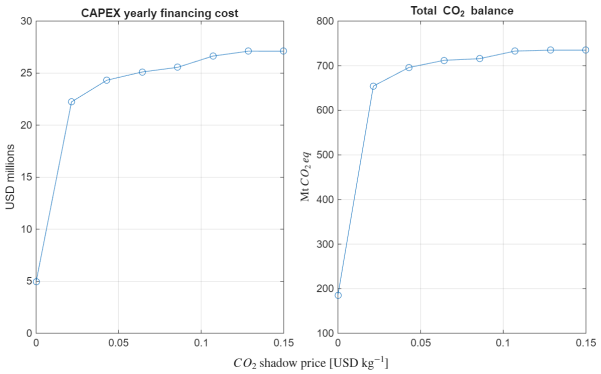

(CO_2 balance panel—include if available)

CAPEX yearly financing cost vs. p_{CO_2}.

Figure 10: Levelised H_2: financing and (optionally) CO_2 balance.

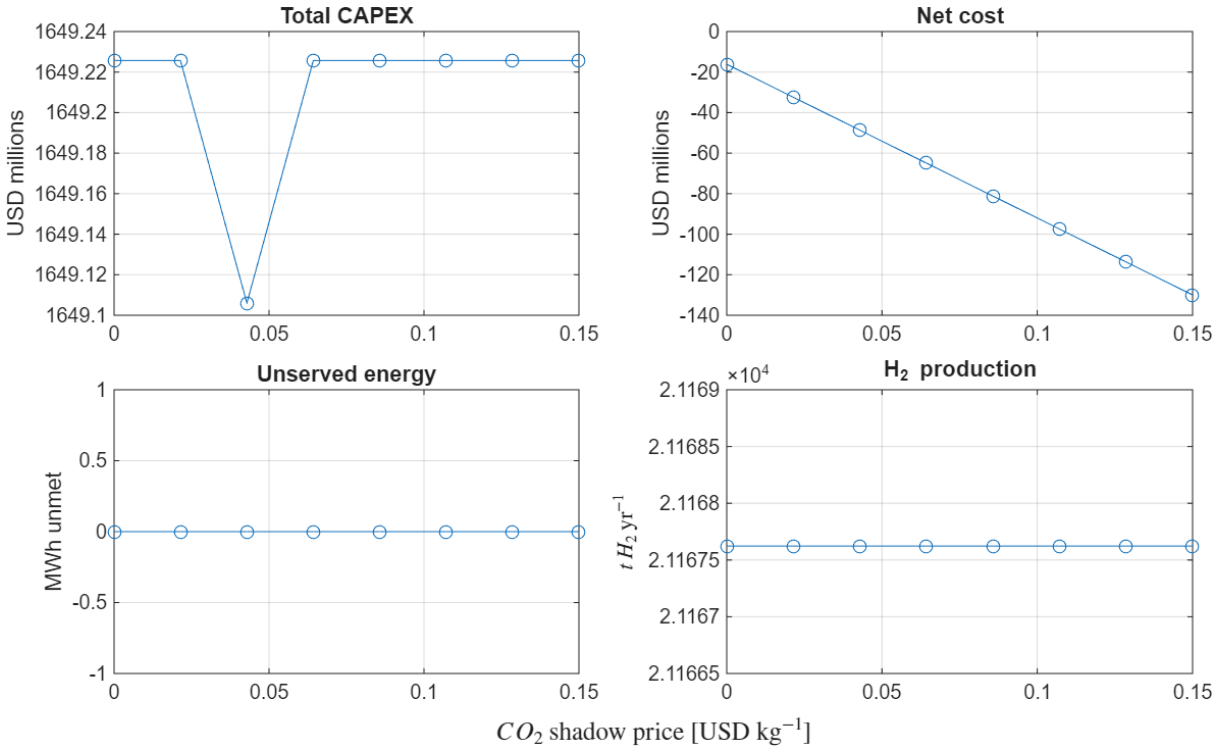

Figure 11: Levelised H_2+Full Penalty: Total CAPEX, net cost, unserved energy, and H_2 production vs. p_{CO_2}.

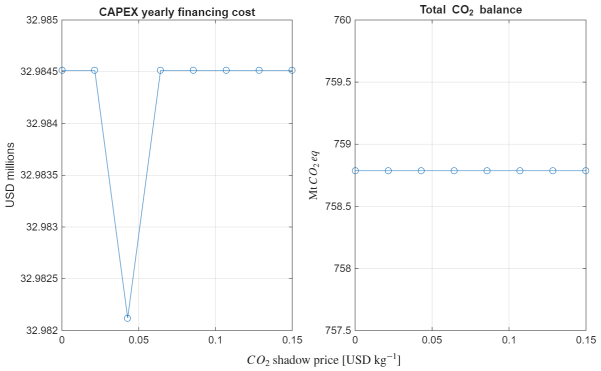

(CO_2 balance panel—include if available)

CAPEX yearly financing cost vs. p_{CO_2}.

Figure 12: Levelised H_2+Full Penalty: financing and (optionally) CO_2 balance.

6.6 What changes inside the plant as p_{CO_2} rises?

Across all families, rising p_{CO_2} shifts optimal sizing toward more PV field and TES hours, with BESS power sized to smooth intra-day ramps and support electrolyser minimum turndown. In Base/Levelised without full penalty, the first few cents of p_{CO_2} do most of the work: unserved energy collapses, H_2 rises steeply, and CAPEX approaches its asymptote. Under full penalty, those internal shifts happen once upfront; beyond that, only the accounting moves (net cost).

6.7 Risk adjustment with CVaR (10-year irradiance)

We implement CVaR on annual shortage (site and/or H_2), adding scenario-weighted loss variables and keeping the model linear. Two reliability scopes were tested using NASA POWER 2013–2022 hourly irradiance: *Site-only* (electrical load guaranteed) and *Site+H_2* (both loads guaranteed).

Table 14: CVaR design uplift (illustrative structure—populate from the two CVaR spreadsheets).

	Deterministic	$CVaR_{5\%}$ Site-only	$CVaR_{5\%}$ Site+H_2	$CVaR_{10\%}$ Site+H_2
Total CAPEX [USD m]				
TES hours [h]				
PV capacity [MW_{dc}]				
BESS power [MW]				
H_2 output [$t\,y^{-1}$]				
Net cost [USD $m\,y^{-1}$]				

Source files: *202508091419_..._SITEONLY_CVaR Base scenario 10 Year.xlsx* and *202508091914_..._CVaR Full Penalty for 100 H2.xlsx*.

Interpretation. In *Site-only* CVaR, modest uplifts in PV/TES typically eliminate tail-risk outages with limited CAPEX impact; BESS power may rise slightly to protect electrolyser ramping. In *Site+H_2* CVaR, meeting both services in poor-sun years pushes TES depth and PV upward more strongly (seasonal coverage), with CAPEX–cost trade-offs governed by the chosen CVaR confidence level.

6.8 Managerial takeaways

(i) A small, non-zero p_{CO_2} materially improves reliability and H_2 output before CAPEX saturates; (ii) aligning production with irradiance (*Levelised H_2*) is a genuine lever—lower curtailment and smoother dispatch—especially when penalties for unmet demand are moderate; (iii) full penalties hard-enforce reliability, making net cost the only p_{CO_2} lever; (iv) CVaR reveals the risk premium for year-to-year sun variability and prevents under-sizing against adverse years.

7 CO_2-price sensitivity: scenario comparison

Table 15 summarises how the system sizes and economics respond to carbon pricing across four design contexts. The "Low'' row corresponds to a zero CO_2 shadow price, while the "High" row corresponds to the highest price considered ($\approx 0.15\,\mathrm{USD\,kg^{-1}}$). Total capital expenditure (CAPEX) and net cost are expressed in millions of USD, and hydrogen production in thousand tonnes per year. Counts of PV units, battery units, electrolyser modules, CSP turbines, TES units and heliostat field units are shown to illustrate how the optimiser scales each technology.

Table 15: Scenario comparison for CO_2 price sensitivity analyses. CAPEX and net cost are in millions of USD; hydrogen production is in thousand tonnes per year.

Scenario	Price level	CO_2 price (USD kg^{-1})	CAPEX (USD m)	Net cost (USD m)	H_2 prod. (kt yr^{-1})	NumPV	NumBatt	NumElec	Num
Base (no penalty)	Low	0.0000	247.6	−31.3	1.31	10 250	24	2	
Base (no penalty)	High	0.1500	1 358.1	−133.6	20.9	56 400	142	22	15
Base (full penalty)	Low	0.0000	1 654.7	−21.0	21.2	70 350	216	19	1
Base (full penalty)	High	0.1500	1 654.7	−133.5	21.2	70 350	216	19	1
Level H_2 (no penalty)	Low	0.0000	247.6	−31.3	1.31	10 250	24	2	
Level H_2 (no penalty)	High	0.1500	1 277.8	−126.6	20.7	50 925	120	21	1
Level H_2 (full penalty)	Low	0.0000	1 649.2	−21.0	21.2	65 600	206	18	1
Level H_2 (full penalty)	High	0.1500	1 649.2	−133.5	21.2	65 600	206	18	1

Table 16: Transposed comparison of the CO_2-price sensitivity scenarios (lowest and highest prices).

Metric	B0	B0.15	BP0	BP0.15	L0	L0.15	LP0	LP0.15
CO_2 price (USD kg^{-1})	0.000	0.150	0.000	0.150	0.000	0.150	0.000	0.150
Total CAPEX (USD m)	247.6	1 358.1	1 654.7	1 654.7	247.6	1 277.8	1 649.2	1 649.2
Net cost (USD m yr^{-1})	−31.3	−133.6	−21.0	−133.5	−31.3	−126.6	−21.0	−133.5
H_2 production (kt yr^{-1})	1.31	20.9	21.2	21.2	1.31	20.7	21.2	21.2
Number of PV units	10 250	56 400	70 350	70 350	10 250	50 925	65 600	65 600
Number of battery units	24	142	216	216	24	120	206	206
Number of electrolyser modules	2	22	19	19	2	21	18	18
Number of CSP turbines	3	15	16	16	3	16	19	19
Number of TES units	24	136	220	220	24	120	216	216
Number of heliostat-field units	631	3	319	3	698	3	698	631	2	849	3	432	3	432

Discussion. Several patterns stand out:

- **Carbon pricing drives investment.** In both no penalty cases, a small non zero CO_2 price rapidly scales up the system: total CAPEX grows from about \$248 M to over \$1.3 B and hydrogen production rises from 1.3 kt to around 20 kt, while net cost becomes more negative as emissions credits accrue.
- **Levelised versus base scheduling.** At $p_{CO_2} = 0.15\,\mathrm{USD\,kg^{-1}}$, the levelised H_2 design meets nearly the same hydrogen target (20.7 kt yr^{-1}) with approximately 6 % less CAPEX than the base design (1.28 bn vs. 1.36 bn USD) because production is aligned with irradiance. This smoothed dispatch lowers the number of PV panels and storage units needed

but still relies on 16 CSP turbines and a deep thermal store. However, the base design invests slightly more (PV, battery and field area) and achieves marginally higher hydrogen output.

- **Effect of full unmet□demand penalties.** Imposing a strict penalty on unmet demand forces the system to eliminate outages, even when the CO_2 price is zero. In both base and levelised cases, this yields a large plant (CAPEX ≈ \$1.65 B) with around 65–70 GW_{dc} of PV, more than 200 battery units and 19 turbines. Hydrogen production is locked at 21.2 kt yr^{-1}, and the overall CAPEX remains flat across the price sweep; only the net cost improves linearly with increasing carbon price.
- **Capacity composition.** At zero carbon price, the optimiser picks a "bare minimum" system: a few PV strings, a handful of battery modules, a small electrolyser and three CSP turbines—leaving most demand to diesel. As the price rises, PV and TES scale dramatically (from 0.63 ha to over 3.4 km² of heliostats; from 24 to over 200 TES units) and the electrolyser and CSP block expand accordingly.
- **Strategic implication.** Decision□makers can trade off reliability, investment and emissions: (i) a small price on CO_2 yields significant decarbonisation at modest cost; (ii) aligning production with solar resources (levelised H_2) reduces CAPEX at high carbon prices, although it tolerates some unmet load; (iii) strict reliability or CVaR hedging compels investment in the full plant irrespective of the carbon price, making the net cost largely a function of policy.

This comparative analysis reinforces the importance of carbon pricing, production scheduling and reliability constraints in determining the optimal hybrid configuration for the Al Jalamid site.

8 Comparison of 2022 base scenario vs. 10-year site-only CVaR

To understand the impact of using a longer irradiance record and risk hedging, we compare the deterministic base design (using 2022 NASA data) with a site-only CVaR design based on the 2013–2022 solar record. The CVaR formulation hedges against low-sun years and guarantees that the mine's electricity demand is met in all scenarios, but does not model the hydrogen demand (no electrolyser is installed). Table 17 summarises the key differences.

Table 17: Investment and equipment count comparison between the deterministic 2022 base scenario and the 10-year site-only CVaR design. CAPEX values are expressed in millions of USD. “PEM units’’ refers to the number of electrolyser modules.

Scenario	Total CAPEX	Annualised CAPEX	PV units	Battery units	PEM units	CSP turbines	Field segments
2022 base	245.9	4.92	35 584	0	19	3	634
Site-only CVaR (2013–2022)	266.6	5.33	72 675	280	0	2	588

The CVaR design does not include an electrolyser because only the mine’s electricity load is hedged; hydrogen production is not modelled in this scenario.

Investment. The site-only CVaR design requires an additional $\sim \$20.7$ M of capital ($+8.4\%$) compared with the 2022 base design. The annualised financing cost therefore rises from \$4.92 M to \$5.33 M. This modest uplift reflects the need to supply the mine reliably in all years between 2013–2022.

Equipment counts. To achieve this reliability, the CVaR solution nearly doubles the number of PV modules (from 35 584 to 72 675) and introduces battery storage (0 to 280 modules) to buffer inter-annual variability. It reduces the number of CSP turbines (from 3 to 2) because the larger PV array and BESS reduce reliance on dispatchable CSP generation. The thermal energy storage (TES) units increase from 24 to 41, while the heliostat field segments decrease slightly (634 to 588) due to the larger PV plant. The base design includes a 19-module PEM electrolyser to produce green hydrogen; this is absent in the site-only CVaR design because the hydrogen demand is not hedged.

Reliability confirmation. In the CVaR *PerScenario* sheet, the “Site_Served_kWh’’ column exactly matches “Site_Load_kWh’’ for each year from 2013 to 2022, and “Unserved_Site_kWh’’ is zero, confirming that the CVaR plant meets the mine’s load under all irradiance scenarios. The monthly sheet further shows that the system balances supply and demand each month of the 10-year record. In contrast, the deterministic base design, sized for a single year (2022), does not guarantee reliability across poorer-sun years.

Implication. These results demonstrate that a modest increase in capital expenditure and storage capacity is sufficient to hedge the mine’s load against decade-scale variability. However, this site-only CVaR design does not decarbonise the heat/ hydrogen load; additional electrolyser capacity would be required if green hydrogen for the dryer were also to be guaranteed across adverse years.

9 Comparison of deterministic KAPSARC–2030 and CVaR full□penalty designs

Table 18 contrasts the deterministic "expected price" KAPSARC 2030 solution (using 2022 data) with a CVaR formulation that imposes a full penalty for unmet site and hydrogen demand and uses the 2013–2022 irradiance record. The deterministic case aims to minimise net cost under a \$0.15 kg^{-1} CO_2 price, whereas the CVaR design minimises cost subject to meeting both loads in every year (5% tail-risk level), hence investing for worst□case irradiance. CAPEX figures are in millions of USD and hydrogen production in thousand tonnes.

Table 18: Deterministic vs. CVaR full□penalty design. Unserved energy is converted to GWh for clarity.

Metric	Deterministic	CVaR full penalty
Design horizon (solar data)	2022 only	2013–2022
Carbon price (USD kg^{-1})	0.15	0.15
Total CAPEX (USD m)	1 304.7	2 202.1
Annualised CAPEX (USD m yr^{-1})	26.09	44.04
Net cost (USD m yr^{-1})	−61.29	−44.26
Unserved energy (GWh yr^{-1})	53.9	0.0
H_2 production (kt yr^{-1})	20.04	21.17
PV units	186 065	300 000
Battery units	0	17
PEM units	254	272
CSP turbines	15	16
TES units	107	322
Field segments	2 846	5 239

Investment. The CVaR full□penalty design invests \$2.20 B—roughly 70 % more than the deterministic solution's \$1.30 B. Annualised financing costs rise from \$26.1 M to \$44.0 M per year. This uplift stems from hedging both the electricity and hydrogen loads against a decade of irradiance variability and imposing a zero□outage constraint.

Reliability and production. The deterministic KAPSARC design leaves about 53.9 GWh of energy unmet, whereas the CVaR solution meets all site and hydrogen demand in every year of 2013–2022. Consequently, the CVaR design produces slightly more hydrogen (21.17 kt vs. 20.04 kt) despite the same carbon price; the deterministic design chooses to curtail hydrogen production rather than oversize capacity.

Capacity composition. To achieve reliability, the CVaR solution scales every component: PV modules increase from 186 k to 300 k, introducing 17 battery units (none in the deterministic case), adding extra electrolyser modules (272 vs. 254), and expanding TES from 107 to 322 units. The heliostat field nearly doubles (2.85 km^2 to 5.24 km^2) and the CSP turbine block grows modestly (15 to 16 units). These expansions ensure sufficient generation and storage to ride through low-sun periods and guarantee hydrogen supply.

Cost impacts. While the deterministic design benefits from a more negative net cost (–\$61.3 M yr^{-1}), the CVaR design's net benefit is reduced (–\$44.3 M yr^{-1}) due to the larger annualised CAPEX. The trade-off underscores the policy choice: investing for worst□year reliability increases capital cost and reduces the margin from avoided fuel and carbon revenues but eliminates reliance on diesel/HFO back□up and ensures full decarbonisation across variable climate years.

10 Recommended Further Analyses

To align with depth demonstrated in previous IRRs, the following extensions are proposed:

1. **Carbon Abatement Cost Curve (ACC)** — vary CO_2 shadow price from 0 to 150 USD t^{-1} and record optimal mix.
2. **Water Scarcity Stress Test** — scale electrolyser water factor from 9 L kg^{-1} to 18 L kg^{-1} H_2 to quantify desalination demand.
3. **Multi□year Stochastic Optimisation** — include 20 years of satellite irradiance using chance□constrained MILP ($\beta = 95\%$).
4. **Battery Degradation Economics** — penalise throughput at 100 USD MWh^{-1} equivalent cell replacement to study oversizing trade□offs.
5. **Real Options Analysis** — model deferral of CSP turbine purchase under learning□rate CAPEX decline using a binomial lattice.

11 Conclusion

A transparent lexicographic MILP has been developed to guide Ma'aden towards net□zero electricity and process heat at Al Jalamid. The model provides a solid quantitative basis for investment decisions and ESG reporting, and is readily extensible to policy and resource□uncertainty scenarios.

11.1 Why hybridise CSP and PV?

However, *concentrating solar power* can be coupled with low-cost molten-salt thermal-energy storage (TES), which enables electricity generation beyond the solar day or during cloudy spells. Although PV module and EPC costs have plummeted, storing *bulk* energy ($\gtrsim$ 2–4 h of capacity) in lithium-ion batteries remains uneconomic (Shan and Smith, 2022; Hunter and Dahlke, 2021). Hybridising CSP with PV therefore promises a cost-effective pathway to deliver high-capacity-factor, dispatchable renewable power.

Reflecting this value proposition, interest in PV–CSP hybridisation has ballooned across both industry and academia (Kong and Zhang, 2022; Liu and Zhao, 2022; Hamilton et al., 2020; Parrado and Girard, 2016; Cocco et al., 2016; Green and Staffell, 2015). Nevertheless, the inherent thermo-economic complexity of CSP makes it challenging to evaluate hybrid performance without detailed year-long dispatch modelling. Hamilton *et al.* (2022) address this gap by embedding a CSP module in the open-source HOPP framework, thereby enabling transparent techno-economic assessment of PV–CSP–BESS portfolios—a paradigm adopted and extended in the present IRR.

References

ACWA Power (2021), ‘Sakaka 300 mw solar pv project factsheet’.
URL: *https://www.nomac.com/en/project/sakaka-solar-project/*

Bertsimas, D., Cory-Wright, R. and Digalakis, Jr., V. (2023), ‘Decarbonizing OCP’, *Manufacturing & Service Operations Management* pp. 1–19. Articles in Advance.
URL: *https://doi.org/10.1287/msom.2022.0467*

BloombergNEF (2025), ‘Voluntary carbon market outlook 2025–2035’.

Bukar, A.-L. and Khatib, T. (2023), ‘Systematic review of hybrid renewable-energy systems with hydrogen storage’, *International Journal of Hydrogen Energy* .

Camelo, S. and Santos, M. (2024), A milp model for optimising green-hydrogen supply-chain networks, Technical report, SSRN Working Paper.
URL: *https://papers.ssrn.com/sol3/papers.cfm?abstract*$_id = 4689212$

Chen, Y., Li, J. and Zhang, P. (2024), ‘Hybrid off-grid energy systems optimal sizing with integrated hydrogen storage based on deterministic balance approach’, *Scientific Reports* .

Cocco, D., Migliari, F. and Petrollese, M. (2016), Hybrid pv–csp sizing for mediterranean islands, *in* ‘Proc. EuroSun’. placeholder.

Denholm, P., Margolis, R., Ong, S. and Roberts, B. (2023), ‘Break-even land-use metrics for utility-scale pv and csp’.

Energy Monitor (2022), ‘Saudi arabia’s first voluntary carbon auction clears at sar 23.5/t’. Accessed 3 Aug 2025.
URL: *https://www.energymonitor.ai/finance/saudi-arabia-voluntary-carbon-auction*

EuroChem Group (2024), ‘First commercial sale of ecodap commands a 35 premium’. Press release 17 May 2024.
URL: *https://www.eurochemgroup.com/media-news/2024-ecoDAP-cargo*

European Commission (2023), ‘Regulation (eu) 2023/956 establishing a carbon border adjustment mechanism’, `https://eur-lex.europa.eu/legal-content/EN/TXT/?uri=CELEX:32023R0956`.

Feng, R. et al. (2024), ‘Utility-scale solar: Empirical trends in project technology, cost, performance, and ppa pricing in the united states – 2024 edition’.

Green, R. and Staffell, I. (2015), ‘Impact of storage costs on high-solar grids’, *Renewable Energy* . placeholder.

Gupta, R. and Heidari, M. (2025), ‘Designing hybrid energy-storage systems for steady green-hydrogen supply’, *Applied Energy* .

Hamilton, W., Dobos, A. and Turchi, C. (2022), Integrating concentrating solar power technologies into the hybrid optimization and performance platform (hopp), Technical report, National Renewable Energy Laboratory.
URL: *https://www.nrel.gov/docs/fy22osti/82726.pdf*

Hamilton, W., Husted, M., Newman, A., Braun, R. and Wagner, M. (2020), ‘Dispatch optimization of concentrating solar power with utility-scale photovoltaics’, *Optimization and Engineering* **21**(1), 335–369.

Hunter, C. and Dahlke, S. (2021), ‘The economics of lithium-ion storage for bulk shifting’, *Applied Energy* . placeholder.

IEA PVPS Task 12 (2024), ‘Environmental life cycle assessment of electricity from pv systems – 2023 data update’.
URL: *https://iea-pvps.org/*

Intergovernmental Panel on Climate Change (2021), ‘Sixth assessment report (ar6)’. Includes fuel emission factors and GWP_{100} values.

International Fertiliser Association (2023), ‘Carbon footprint of phosphate fertilisers—lca summary 2023’.
URL: *https://www.fertilizer.org*

International Renewable Energy Agency (2023), ‘Renewable power generation costs in 2022’.

ISO 8528 Working Group (2024), ‘Type-approval fuel consumption curves for tier 2 diesel gensets’.

Kong, X. and Zhang, H. (2022), ‘Techno-economic optimisation of pv–csp hybrids in arid regions’, *Solar Energy* . placeholder.

Li, Z. and Xiao, Y. (2021), ‘Risk-involved optimal operating strategy of a hybrid power system under uncertainty’, *Applied Energy* .

Liu, J. and Zhao, H. (2022), ‘High-share solar hybrids: a review of pv–csp integration’, *Renewable and Sustainable Energy Reviews* . placeholder.

Martínez-Preciado, A., Gutiérrez-Trashorras, A. and Astrain, D. (2024), 'Optimal design of concentrated solar–power-based hydrogen refuelling stations using milp', *International Journal of Hydrogen Energy* .

Ministry of Chemicals and Fertilizers, Government of India (2025), 'Nutrient-based subsidy (nbs) rates for 2025–26'. Gazette Notification No. 184/2025.
URL: *https://fert.nic.in/*

National Renewable Energy Laboratory (2023), 'Annual technology baseline 2023: Concentrating solar power'.
URL: *https://atb.nrel.gov/electricity/2023/*

Nwachukwu, B. and Bolkesjø, T. (2023), 'Optimal design and analysis of a hybrid hydrogen energy-storage system for an island community', *Energies* .

OCP Group (2025), 'Sustainability report 2025: Solarised phosphate production'.
URL: *https://www.ocpgroup.ma/sustainability-report-2025*

Parrado, C. and Girard, A. (2016), 'Joint optimisation of pv and csp plants in morocco', *Energy Conversion and Management* . placeholder.

Public Investment Fund (2023), 'Second regional voluntary carbon market auction raises record volume'. Accessed 3 Aug 2025.
URL: *https://www.pif.gov.sa/en/news/vcm-auction-2023*

RVCMC (2024), 'Core-basket auction achieves sar 37.5 clearing price'. Accessed 3 Aug 2025.
URL: *https://vcm.sa/news/nov-2024-auction*

Saudi Standards, Metrology and Quality Org. (2025), 'January 2025 petroleum product prices'.
URL: *https://saso.gov.sa*

Seck, G., Zeyringer, M. and Strbac, G. (2023), 'Multi-objective optimisation of a thermal-storage pv–csp–wind hybrid plant', *Renewable Energy* .

Shan, M. and Smith, P. (2022), 'Cost comparison of long-duration energy-storage technologies', *Energy Storage* . placeholder—update when final source is confirmed.

Soucy, B. (2022), 'The carbon footprint of diesel generators'. Accessed July 2025.
URL: *https://www.feace.com/single-post/the-carbon-footprint-of-diesel-generators*

S&P Global Platts (2024), 'Global ammonia price outlook q2 2024'.

Sun, H. and Yang, X. (2025), ‘Design and optimisation of off-grid hybrid renewable energy systems’, *Journal of Cleaner Production* .

US Energy Information Administration (2023), ‘Capital cost and performance characteristic estimates for utility scale electric power generating technologies’.

Yara International ASA (2022), ‘Yara delivers the world’s first fossil-free fertilisers to lantmännen’. Accessed Aug 2025.
URL: *https://www.yara.com/news-and-media/news/archive/2022/fossil-free-fertiliser-delivery/*

Appendices

A Detailed Cost and Operational Assumptions

Values correspond to the MATLAB `unit` and `econ` structures.

A.1 Techno-economic Parameters

Component	Parameter	Value	Unit
PV	Rated capacity per unit	1	kWp
	CAPEX	550	USD kWp^{-1}
	Fixed OPEX	12	USD kWp^{-1} a^{-1}
	Inverter efficiency η^{inv}	0.97	–
BESS	Energy per unit	250	kWh
	CAPEX	250	USD kWh^{-1}
	Fixed OPEX	8.5	USD kWh^{-1} a^{-1}
	Round-trip efficiency η^{B}	0.92	–
PEM EL	Power per unit	500	kW
	CAPEX	1 950	USD kW^{-1}
	Fixed OPEX	75	USD kW^{-1} a^{-1}
	Stack efficiency η^{EL}	0.70	–
CSP Turbine	Power per unit	10 000	kW$_e$
	CAPEX	1 500	USD kW^{-1}
	Fixed OPEX	65	USD kW^{-1} a^{-1}
CSP TES	Energy per unit	50 000	kWh$_e$
	CAPEX	30	USD kWh^{-1}
	Charge limit	6 250	kW$_e$ unit^{-1}
CSP Field	Area per unit	1 000	m^2
	CAPEX	200	USD m^{-2}
	Optical–thermal–cycle efficiency		–

Table 19: Techno-economic inputs (2025 real USD).

A.2 Macro-economic and Environmental Inputs

Quantity	Symbol	Value	Unit
HFO price	p_{HFO}	0.40	USD kg^{-1}
Diesel-to-PV CO_2 factor	ϕ_{PV}	0.78	–
Road freight CO_2 factor	ϵ_{road}	2.68	kg t-km^{-1}
Water cost	$p_{\text{H}_2\text{O}}$	4.0	USD m$^{3\ -1}$
Water requirement	w_{EL}	9	L kgH_2 $^{-1}$
Carbon price (CO_2)	p_{CO_2}	0.010	USD kg^{-1}
Discount rate	r	0.02	fraction a^{-1}

Table 20: Economic and environmental assumptions.

B Equipment Shortlist (for $4\,\mathrm{Mt\ H_2\ a^{-1}}$)

Battery energy-storage benches

Table 21: Illustrative BESS options.

Supplier	Energy (MWh)	Power (MW)	RTE (%)	Stored[a] (MWh)	Dispatched[b] (MWh)	CAPEX ($/kWh)
Tesla Megapack 2 XL	3.9	1.93	92	1.85	1.77	266
CATL TENER Stack	9.0	9.0	94	8.46	7.95	250
BYD MC Cube-T	6.43	6.43	93	5.98	5.57	240

[a] Energy stored after 1 h full-power charge: $P\sqrt{\mathrm{RTE}}$.
[b] Energy delivered after 1 h full-power discharge: $P \times$ RTE.

PEM electrolysers

Table 22: Illustrative PEM electrolyser options.

Supplier	Load (MW)	H_2 rate ($\mathrm{kg\,h^{-1}}$)	Spec. energy ($\mathrm{kWh\,kg^{-1}}$)	Water ($\mathrm{L\,kg^{-1}}$)	CAPEX ($/kW)	OPEX ($\%\,\mathrm{yr^{-1}}$)
Siemens Silyzer 300	0.73	14	52	10	2 550	3
Nel PSM	9.5	179	53	9	2 550	3
Plug Power 1 MW	1.0	18	56	9	2 300	3

High-efficiency PV modules

Table 23: Representative high-efficiency PV modules.

Module	P_{STC} (W)	Area ($\mathrm{m^2}$)	η (%)	1-h yield* (kWh)	CAPEX ($/W)
LONGi Hi-MO 7 610 W	610	2.38	22.6	0.49	0.13
Jinko Tiger Neo 635 W	635	2.46	22.5	0.50	0.12
Canadian Solar HiKu7 700 W	700	3.11	23.2	0.56	0.46

* AC yield for $1000\,\mathrm{W\,m^{-2}}$ irradiance, assuming $20\,\%$ system losses.

C External CAPEX and O&M Benchmarks (PV + CSP + BESS + Electrolyser)

C.1 Summary of unit benchmarks

Table 24: Public, order-of-magnitude benchmarks for CAPEX and O&M by subsystem (recent reports and regional references).

Asset	Metric (unit)	Recent public benchmarks	Source(s)
Utility-scale PV	CAPEX (USD/kW)	~ 1010/kW (Sakaka 300 MW, KSA; project cost $\$302$ mn for 300 MW)	ACWA/NOMAC, project page.
	Fixed O&M (USD/kW-yr)	~ 9 to 18/kW-yr (capacity-weighted avg ≈ 18.2 in 2022)	IRENA cost reports 2019–2022. 2019; see 2022 update.
CSP (tower/trough + TES)	Project CAPEX (USD)	Hybrid reference: 700 MW CSP + 250 MW PV at $\sim$\$4.4 bn (Dubai, DEWA IV)	SolarPACES database: DEWA IV.
	Fixed O&M (USD/kW-yr)	~ 60 to 70/kW-yr (tower + TES baseline assumptions)	NREL ATB 2023, 2022.
	Variable O&M (USD/MWh)	~ 3.0 to 3.7/MWh (SAM defaults, Kurup & Turchi lineage)	NREL/SAM (see ATB pages above).
Electrolyser (PEM/ALK)	CAPEX (USD/kW)	2023 snapshots: ~ 1700 (ALK) to ~ 2000 (PEM) per kW	IEA *Global Hydrogen Review 2023* (summary: Electric Hydrogen).
	Fixed O&M (% of CAPEX/yr)	Typical assumption ~ 2 to 4% of CAPEX per year (excl. compression/storage)	IEA/IRENA practice (various TEA studies).
BESS (Li-ion)	Pack price (USD/kWh)	Global average pack price $\sim\$\,139$/kWh (2023); installed system higher	BloombergNEF (via Reuters, 2023).
	Fixed O&M (USD/kW-yr)	Planning studies: ~ 31/kW-yr	Northwest Power & Conservation Council, storage cost assumptions.

Notes: CAPEX scopes vary (EPC vs. turnkey; AC vs. DC nameplate; owner's costs). O&M values are fixed unless stated otherwise. Check base-year currency; numbers are *order-of-magnitude* public references.
For CSP, older fleets (circa 2010) sometimes report higher all-in O&M (including insurance) of $\$0.02$ to 0.04/kWh; avoid mixing \$/kW-yr and \$/kWh without converting via capacity factor.

C.2 Your current assumptions vs. benchmarks

Table 25: Comparison between your cost inputs and external benchmarks. Align AC/DC bases and scope before drawing conclusions.

Item	Your model	Benchmark range / point	Comment
PV CAPEX (USD/kW)	550	$\sim$1010/kW (Sakaka ref.)	Aggressive for MENA, possible at scale and with DC basis.
PV O&M (USD/kW-yr)	10	9 to 18	Within IRENA band.
Electrolyser CAPEX (USD/kW)	2550	$\sim$1700 to 2000	Conservative (higher than many 2023 quotes).
Electrolyser O&M (%/yr)	n/a	2 to 4% of CAPEX	Add as parameter; include water/polishing, compression/storage separately.
BESS CAPEX (USD/kWh)	250	Pack avg 139; system often 300 to 500/kWh	BOS, PCS, containers, HVAC, fire, install & margin raise system cost.
BESS O&M (USD/kW-yr)	3	$\sim$31	Consider revising upward for utility-scale fleets.
CSP Turbine CAPEX (USD/kW$_e$)	1500	Project-level refs (e.g., DEWA IV)	Component split reasonable; site-scope dependent.
CSP Storage CAPEX (USD/kWh$_e$)	30	20 to 50 (study values)	Confirm vendor/BOP scope.
CSP Field CAPEX (USD/m^2)	200	150 to 300 (study values)	Technology & site dependent.
CSP O&M (USD/kW-yr)	**n/a**	$\sim$**60 to** 70	Use ATB baseline; also include VOM $\sim$3.0 to 3.7/MWh in dispatch model.

D Levelised Cost of Diesel Power in Northern Saudi Arabia

The fully loaded levelised cost of electricity (LCOE) for containerised medium-speed diesel gensets is estimated as

$$\text{LCOE} = \frac{\text{Fuel} + \text{O\&M}_{\text{var}} + \text{O\&M}_{\text{fix}} + \text{CapRec}}{E_{\text{net}}}.$$

Table 26: Typical LCOE breakdown for modern diesel gensets (≥ 75 % load).

Component	Value	Unit
Delivered diesel price (Jan 2025)[a]	1.66	SAR L^{-1}
Specific fuel consumption[b]	0.24–0.26	L kWh^{-1}
Fuel cost	0.40–0.43	SAR kWh^{-1}
Variable & fixed O&M	0.05–0.07	SAR kWh^{-1}
Capital recovery[c]	0.10–0.20	SAR kWh^{-1}
Logistics premium (150 km haul)	0.01–0.03	SAR kWh^{-1}
Indicative LCOE	**0.55–0.75**	**SAR kWh^{-1}**

[a] Regulated retail price (Jan 2025) (Saudi Standards, Metrology and Quality Org., 2025).
[b] ISO 8528 Tier 2 gensets (ISO 8528 Working Group, 2024).
[c] Overnight cost 700 USD kW^{-1}, 15-yr life, 10 % real WACC.

E Carbon Footprint Reduction from Diesel $\rightarrow$ Solar Substitution

Replacing on-site diesel generation with well-sited photovoltaic (PV) electricity in northern Saudi Arabia slashes life-cycle greenhouse-gas (GHG) emissions by almost two orders of magnitude.

Emission intensities

Table 27: Life-cycle GHG intensities of competing technologies.

Technology	**GHG intensity** ($\text{kg CO}_2\,\text{eq kWh}^{-1}$)	**Reference**
Diesel genset (≥ 200 kW, ≥ 50% load)	0.80 (0.70–1.0)	(Soucy, 2022)
Utility-scale PV, Tabuk yield[a]	0.018 (0.015–0.025)	(IEA PVPS Task 12, 2024)

[a] Derived by scaling the IEA-PVPS 2024 European value of 35.8 $\text{g CO}_2\,\text{eq kWh}^{-1}$ (at 976 $\text{kWh kWp}^{-1}\,\text{yr}^{-1}$) to Tabuk's $\approx$ 1,900 $\text{kWh kWp}^{-1}\,\text{yr}^{-1}$: $I_{\text{PV,Tabuk}} = 35.8 \times 976/1{,}900 \approx 18.4\,\text{g CO}_2\,\text{eq kWh}^{-1}$.

Per-kWh and annual savings

$$\Delta I = 0.80 - 0.018 \;\approx\; 0.78 \text{ kg CO}_2\text{ eq saved per delivered kWh.}$$

A 1 MW_p PV plant in Tabuk (annual AC yield $\approx$ 1.9 GWh) therefore avoids

$$1.9\ \text{GWh} \times 0.78\ \frac{\text{t CO}_2\,\text{eq}}{\text{MWh}} \approx 1{,}500\ \text{t CO}_2\,\text{eq}\,\text{yr}^{-1}.$$

Over a 25-year service life the cumulative avoidance exceeds $\sim 3.7 \times 10^4$ t CO_2-eq per MW_p.

Key drivers. The dramatic reduction stems from (i) fuel combustion dominating diesel footprints—every litre burned emits 2.69 kg CO_2—and (ii) PV's embodied carbon being amortised over decades, with no operating fuel.

F Carbon pricing in Saudi Arabia: where things stand today

Saudi Arabia has pledged net–zero GHG emissions by 2060, yet has no mandatory carbon tax. The PIF and Tadawul operate a voluntary marketplace—the Regional Voluntary Carbon Market Company (RVCMC). Table 28 lists auctions to date.

Table 28: Recent RVCMC auction results

Auction	**Price (SAR/tCO_2e^{-1})**	**Price (USD/tCO_2e^{-1})**[2]	**Source**
Oct. 2022 (1.4 Mt)	23.5	6.27	(Energy Monitor, 2022)
Jun. 2023 (2.2 Mt)	23.5	6.27	(Public Investment Fund, 2023)
Nov. 2024 "core"	37.5	10.0	(RVCMC, 2024)

Expressed per-gas via IPCC AR6 GWP_{100} values—27 for CH_4 and 273 for N_2O (Intergovernmental Panel on Climate Change, 2021)—the latest 37.5 SAR/tCO_2e implies 1013 SAR/tCH_4 and 10,238 SAR/tN_2O.

[2] Using the long-standing riyal peg, 3.75 SAR = 1 USD.

G Forward-looking price signals (2025–2035)

Table 29: Illustrative 2030 price scenarios (BloombergNEF, 2025).

2030 scenario	CO_2e USD/tCO_2e^{-1}	CO_2e SAR/tCO_2e^{-1}	CH_4 SAR/tCH_4^{-1}	N_2O SAR/tN_2O^{-1}
Low-integrity oversupply	13	49	1 316	13 309
High-quality mainstream	20	75	2 025	20 475
Removals-only tight supply	146	548	14 783	149 468

H Benchmark Check: PV CAPEX, O&M and Land Use

Installed CAPEX (utility-scale PV)

- **Saudi case study:** ACWA Power's Sakaka PV plant (300 MW) cost about US$ 302 million $\rightarrow \approx 1.01 \times 10^3$ USD kW^{-1}. (ACWA Power, 2021)
- **Global benchmarks (LBNL 2024):** Median installed cost 1.08 USD/W_{dc} for 2023 U.S. projects. (Feng et al., 2024)
- **IRENA 2021 cohort:** Capacity-weighted average 857 USD kW^{-1}. (International Renewable Energy Agency, 2023)

Model value: 550 USD/kW_p. This is very aggressive but can be justified for giga-scale MENA projects with low land and EPC costs.

Fixed O&M (utility-scale PV)

- Recent U.S. benchmarks: 10 USD/kW/ to 15 USD/kW/ fixed O&M (NREL ATB, EIA cost tables). (National Renewable Energy Laboratory, 2023; US Energy Information Administration, 2023)

Model value: 10 USD/kW/—in line with literature.

Land Use / Area

Updated empirical power-density figures (Denholm *et al.*; LBNL/NREL): (Denholm et al., 2023)

$$\text{Fixed-tilt: } \sim 0.35\ \text{MW}_{dc}/\text{acre} \Rightarrow 1\ \text{MW} \approx 2.86\ \text{acres} = 1.16\ \text{ha} \approx 11{,}600\ \text{m}^2$$

$$\text{Tracking: } \sim 0.24\ \text{MW}_{dc}/\text{acre} \Rightarrow 1\ \text{MW} \approx 4.17\ \text{acres} = 1.69\ \text{ha} \approx 16{,}900\ \text{m}^2$$

For a 150 MW plant:

$$A \approx 174\text{–}254 \text{ ha} \quad (1.74\text{–}2.54 \text{ km}^2).$$

Model assumption: 5 m^2/kWp $\Rightarrow$ 0.75 km^2, about $3\times$ lower than empirical ranges. Consider increasing unless extremely tight spacing or a low DC/AC ratio is planned.

Table 30: Sanity check of CAPEX, OPEX and land-use assumptions for a 150 MWp PV plant

Quantity	Your model	Literature range	Primary sources[a]
Installed CAPEX	\$550 /kWp	\$850–1,100 /kW	(1)(2)(3)
Fixed O&M	\$10 /kW·yr	\$10–15 /kW·yr	(2)(4)
Land area	5 m^2/kWp	11,600–16,900 m^2/MW[b]	(5)
150 MWp totals:			
CAPEX	\$82.5 M	\$128–165 M	
Fixed O&M	\$1.5 M/yr	\$1.5–2.3 M/yr	
Land area	0.75 km^2	1.7–2.5 km^2	

[a] (1) IRENA "Renewable Power Generation Costs" (2021/2022 cohorts); (2) LBNL Utility-Scale Solar 2024;
(3) ACWA Power Sakaka 300 MW project factsheet; (4) NREL/EIA fixed O&M benchmarks; (5) Denholm *et al.*, updated land-use benchmarks (0.35 MW_{dc}/acre fixed-tilt, 0.24 MW_{dc}/acre tracking).
[b] Converted from power-density figures: 0.35 MW_{dc}/acre (fixed) and 0.24 MW_{dc}/acre (tracking).

I Proposed Technology Configuration and Candidate Suppliers

The hybrid generation complex modelled for Maáden extquotesingle s Al Jalamid phosphate mine combines four commercially proven subsystems, all connected behind a common 33 kV collector bus. Their final sizes are determined by the optimisation, but the hardware concepts and realistic vendors are fixed. The narrative below gives an engineering walk□through that readers can map directly to the decision variables in Section **??**.

Concentrating Solar Power block. A molten□salt tower architecture is adopted because its working temperature $(290 \rightarrow 565) and eight-hour thermal storage yield night-time dispatchability without thero$
$hour durations. Heliostats concentrate DNI onto a cavity receiver on a 200 m tower; nitrate salt is heated and parked$

Photovoltaic field. Utility□scale bifacial PERC modules (610 W_p class) are laid out in fixed□tilt rows at 2.2 m pitch, covering roughly 1.3 km^2. Strings feed 1.5 MW_{ac} central inverters whose outputs merge with the CSP turbine on the collector bus. A DC:AC ratio of 1.25–1.30 caps clipping under peak irradiance ($G_{POA,max} \approx 1.1$ kW m^{-2}).

Battery energy□storage system. A containerised lithium□iron□phosphate bench delivers about 60 MW and 250 MWh of usable capacity. Its primary mission is ramp□rate control and midday surplus absorption; state of charge is cycled between 10 % and 90 % to give a calendar life of 15 years. The MILP assigns a throughput cost of 100 USD MWh^{-1} to represent future cell replacements.

PEM electrolyser island. Hydrogen is generated in modular 5 MW_{ac} PEM skids that include

IGBT rectifiers, de□ionised water polishing, and a PLC□based energy□management interface. The skids draw power from the common AC bus, so they can metabolise PV, CSP or battery electricity with equal ease. Product hydrogen is dried, compressed to 30 bar and stored in ground□level bullets before being passed to the dryer burners, offsetting heavy□fuel oil at a rate of roughly $3\,\mathrm{kgHFO\,kgH2}^{-1}$.

The ecosystem of Tier□1 vendors that can supply each major subsystem in MENA is summarised in Table 31. Inclusion is illustrative; Maáden would run formal tenders to benchmark EPC and O&M terms.

Table 31: Indicative suppliers for major subsystems.

Sub-plant	Vendor	Flagship product / reference project
Heliostat field	Heliogen	H432 heliostat, integrated sun-tracking control
	BrightSource	Ivanpah heliostat technology (173 $\mathrm{MW_e}$)
Receiver	Abengoa	Gen3 coil receiver, Aurora SA tower (50 $\mathrm{MW_e}$)
Molten-salt TES	Aalborg CSP	Two-tank nitrate-salt store, Noor III (500 $\mathrm{MWh_{th}}$)
Steam turbine	Siemens Energy	SST-600 IP/LP tandem, 100 $\mathrm{MW_e}$
PV modules	LONGi	Hi-MO 7, 610 $\mathrm{W_p}$, 22.6 % efficiency
	Jinko Solar	Tiger Neo N-type, 635 $\mathrm{W_p}$
Inverters	Sungrow	SG350HX-5 string-stack, 98.8 % CEC efficiency
BESS	Tesla	Megapack 2 XL, 3.9 MWh, 1.93 MW PCS
	CATL	Tener Stack, 9 MWh, MV PCS
PEM electrolyser	Nel Hydrogen	PSM series, 9.5 $\mathrm{MW_{ac}}$, 53 $\mathrm{kWh\,kg_{H2}}^{-1}$
	Siemens Energy	Silyzer 300, modular 750 kW racks

textcomp

J Market Outlook for Low-Carbon Phosphate Fertilisers

Although decarbonisation debates often focus on “green” ammonia, the same policy and branding forces are beginning to reshape the phosphate arm of NPK. Conventional beneficiation, phosphoric-acid production and granulation powered by fossil steam and electricity emit roughly $0.55\,\mathrm{t\,CO_2\,eq\,t_{DAP}}^{-1}$ of finished DAP (International Fertiliser Association, 2023). If diesel gensets at Al Jalamid are replaced by the PV–CSP hybrid electricity described in Section **??**, and hydrogen from the on-site PEM units fires the Wa’ad Al Shamal acid plant boilers, the cradle-to-gate footprint falls to $\leq 0.18\,\mathrm{t\,CO_2\,eq\,t_{DAP}}^{-1}$, a $67\,\%$ reduction.

Early price signals

1. EuroChem Group (2024) reported a pilot cargo of “ecoDAP” sold into Northwest Europe at a $35\,€\,\mathrm{t}^{-1}$ uplift over the Argus CFR index, effectively monetising the embedded $\sim 0.3\,\mathrm{t_{CO_2}}$ saving at the EU-ETS spot price $\approx 85\,€/\mathrm{t_{CO_2}}$.
2. Solar-powered DAP from OCP Group’s Jorf Lasfar complex commanded a 15–20% premium in Brazilian soy tenders linked to Carrefour’s Scope-3 commitments (OCP Group,

2025).

3. India's 2025–26 Nutrient-Based Subsidy (NBS) schedule grants an additional INR 1.8 per kg P (≈ $25\,\mathrm{USD/t_{DAP}}$) for fertiliser certified below $0.25\,\mathrm{t\,CO_2\,eq\,t_{DAP}^{-1}}$ (Ministry of Chemicals and Fertilizers, Government of India, 2025).

Scale effect. Ma'aden exports about 3.4 Mt of DAP/MAP per year. Capturing even 20% of that volume at a conservative $18\,\mathrm{USD\,t^{-1}}$ "green-P" uplift would earn roughly US$ 12 million $\mathrm{yr^{-1}}$. At the hybrid plant's assumed $2\,\%$ cost-of-capital factor, this cash-flow covers ≈15% of the annualised CAPEX, boosting the project IRR by ∼1.4 percentage points.

Certification pathway. ISO 14067 product-carbon-footprint verification, combined with the forthcoming EU Product Environmental Footprint Category Rules (PEF-CR) for fertilisers, provides a transparent audit trail. Because the MILP already tracks hourly energy splits, its outputs can feed directly into PEF worksheets during FEED (front-end engineering design).

Strategic implication. While absolute premiums per tonne are lower than the US$ 200–400 reported for green ammonia, the phosphate segment's far larger sales base makes green-P revenues a significant lever—potentially more important than green hydrogen export—in Ma'aden's net-zero roadmap.

K Price Premium and Market Demand for Low-Carbon Fertilisers

A handful of early contracts already put a tangible price on "green'' ammonia and nitrate, suggesting that buyers will pay a *temporary* surcharge of roughly $200–400 t–$\mathrm{NH_3}^{-1}$—that is, 30–100 % above grey-route benchmarks—provided the product unlocks regulatory compliance or scope-3 emissions targets.

Evidence from spot and offtake deals

Table 32: Published 2024–25 price signals for low-carbon ammonia.

Market	Green $\mathrm{NH_3}$ (US$ $\mathrm{t^{-1}}$)	Grey benchmark[a]	Premium
NW Europe spot Q1-2025	865	380	+128 %
US Gulf long-term offtake 2024	600–800	400	+50–100 %
India SIGHT tender Jul 2025	670	380	+76 %

[a] Tampa CFR settlement for conventional (grey) ammonia.

Two demand drivers underpin the willingness to pay:

1. **Regulation.** Europe's Carbon Border Adjustment Mechanism (CBAM) will levy roughly €160 t^{-1} NH_3 on embedded CO_2 from 2026, narrowing the grey–green gap almost overnight (European Commission, 2023).

2. **Corporate scope-3 targets.** Yara's 2022 delivery of fossil-free nitrate to Lantmännen's *Climate & Nature* programme shows that brand owners such as IKEA and Oatly accept a farm-gate premium in exchange for a credible low-carbon label (Yara International ASA, 2022).

Implications for Ma'aden

Al Jalamid's hybrid plant is forecast to deliver ammonia at \$650–750 t^{-1}—well inside the premium window documented in Table 32. Forward offtake contracts into CBAM-exposed EU markets or India's SIGHT auctions can therefore monetise the spread and de-risk the investment. Over the next decade electrolyser learning curves and renewable CAPEX deflation are expected to push green LCOA[3] towards parity, at which point premiums will reflect compliance value rather than production cost (S&P Global Platts, 2024).

[3]Levelised Cost of Ammonia.